

Galactic rotation curves in brane world models

L. Á. Gergely^{1,2*}, T. Harko^{3†}, M. Dwornik^{1,2‡}, G. Kupa^{4§}, Z. Keresztes^{1,2¶}

¹*Department of Theoretical Physics, University of Szeged, Tisza Lajos krt 84-86, Szeged 6720, Hungary*

²*Department of Experimental Physics, University of Szeged, Dóm Tér 9, Szeged 6720, Hungary*

³*Department of Physics and Center for Theoretical and Computational Physics, The University of Hong Kong, Pok Fu Lam Road, Hong Kong, Hong Kong SAR, P. R. China*

⁴*Weizmann Institute of Science, Rehovot 76100, Israel*

28 December 2021

ABSTRACT

In the braneworld scenario the four dimensional effective Einstein equation has extra source terms, which arise from the embedding of the 3-brane in the bulk. These non-local effects, generated by the free gravitational field of the bulk, may provide an explanation for the dynamics of the neutral hydrogen clouds at large distances from the galactic center, which is usually explained by postulating the existence of the dark matter. In the present paper we consider the asymptotic behavior of the galactic rotation curves in the brane world models, and we compare the theoretical results with observations of both High Surface Brightness and Low Surface Brightness galaxies. For the chosen sample of galaxies we determine first the baryonic parameters by fitting the photometric data to the adopted galaxy model; then we test the hypothesis of the Weyl fluid acting as dark matter on the chosen sample of spiral galaxies by fitting the tangential velocity equation of the combined baryonic-Weyl model to the rotation curves. We give an analytical expression for the rotational velocity of a test particle on a stable circular orbit in the exterior region to a galaxy, with Weyl fluid contributions included. The model parameter ranges for which the χ^2 test provides agreement (within 1σ confidence level) with observations on the velocity fields of the chosen galaxy sample are then determined. There is a good agreement between the theoretical predictions and observations, showing that extra-dimensional models can be effectively used as a viable alternative to the standard dark matter paradigm.

Key words: cosmology: dark matter – galaxies: haloes – gravitation: relativistic processes.

1 INTRODUCTION

Gravitational effects which require more matter than what is visible can be explained in terms of a mysterious dark matter, the nature of which remains a long-standing problem in modern astrophysics. Two important observational issues, the behavior of the galactic rotation curves and the mass discrepancy in clusters of galaxies, led to the necessity of considering the existence of dark matter both at galactic and extra-galactic scales.

The rotation curves of spiral galaxies (Binney & Tremaine 1987; Persic et al. 1996; Boriello & Salucci 2001) are among the best evidences

showing the problems Newtonian gravity and/or standard general relativity have to face on the galactic/intergalactic scale. In these galaxies neutral hydrogen clouds are observed at large distances from the center, much beyond the extent of the luminous matter. Since these clouds move in circular orbits with velocity $v_{tg}(r)$, the orbits are maintained by the balance between the centrifugal acceleration v_{tg}^2/r and the gravitational attraction $GM(r)/r^2$ of the total mass $M(r)$ contained within the orbit. This allows the expression of the mass profile of the galaxy in the form $M(r) = rv_{tg}^2/G$.

Observations show that the rotational velocities increase near the center of the galaxy, in agreement with the theory, but then remain nearly constant at a value of $v_{tg\infty} \sim 200 - 300$ km/s (Binney & Tremaine 1987), which leads to a mass profile $M(r) = rv_{tg\infty}^2/G$. Consequently, the mass within a distance r from the center of the galaxy increases linearly with r , even at large distances where very little luminous matter has been detected.

* E-mail: gergely@physx.u-szeged.hu

† E-mail: harko@hkucc.hku.hk

‡ E-mail: marek@titan.physx.u-szeged.hu

§ E-mail: gabor.kupa@weizmann.ac.il

¶ E-mail: zkeresztes@titan.physx.u-szeged.hu

The second astrophysical evidence for dark matter comes from the study of the clusters of galaxies. The total mass of a cluster can be estimated in two ways. Knowing the motions of its member galaxies Giovanelli et al. (1994), the virial theorem gives one estimate, M_{VT} , say. The second is obtained by separately estimating the mass of the individual members, and summing up these masses, to give a total baryonic mass M_B . Almost without exception it is found that M_{VT} is considerably larger than M_B , $M_{VT} > M_B$, typical values of M_{VT}/M_B being about 20-30 (Binney & Tremaine 1987).

This behavior of the galactic rotation curves and of the virial mass of galaxy clusters is usually explained by postulating the existence of some dark (invisible) matter, distributed in a spherical halo around the galaxies. The dark matter is assumed to be a cold, pressure-less medium. There are many possible candidates for dark matter, the most popular ones being the weakly interacting massive particles (WIMP) (for a review of the particle physics aspects of the dark matter see Overduin & Wesson (2004). Their interaction cross sections with normal baryonic matter, while extremely small, are expected to be non-zero, and we may expect to detect them directly. Models based on right-handed (sterile) neutrinos (Biermann & Kusenko 2006; Munyaneza & Biermann 2006) as a form of warm dark matter were also advanced.

It has also been suggested that the dark matter in the Universe might be composed of super-heavy particles, with mass $\geq 10^{10}$ GeV. But observational results show that the dark matter can be composed of super-heavy particles only if these interact weakly with normal matter, or if their mass is above 10^{15} GeV (Albuquerque & Baudis 2003). Scalar fields or other long range coherent fields coupled to gravity have also intensively been used to model galactic dark matter (Fuchs & Mielke 2004; Hernandez et al. 2004; Giannios 2005; Guzmán & Ureña-López 2006; Bernal & Guzman 2006; Briscese 2011; Harko 2011).

However, up to now no non-gravitational evidence for dark matter has been found, and no direct evidence or annihilation radiation from it has been observed yet.

Therefore, it seems that the possibility that Einstein's (and the Newtonian) theory of gravity breaks down at the scale of galaxies cannot be excluded *a priori*. Several theoretical models, based on a modification of Newton's law or of general relativity, have been proposed to explain the behavior of the galactic rotation curves (Milgrom 1983; Sanders 1984; Moffat & Sokolov 1996; Mannheim 1997; Roberts 2004; Böhmer & Harko 2007a; Böhmer & Harko 2007b; Bertolami et al. 2007; Böhmer et al. 2008; Bekenstein 2004; Brownstein & Moffat 2006).

The idea of embedding our Universe in a higher dimensional space has attracted a considerable interest recently, due to the proposal by Randall and Sundrum (Randall & Sundrum 1999a,b) that our four-dimensional (4D) space-time is a three-brane, embedded in a 5D space-time (the bulk). According to the brane world scenario, the physical fields (electromagnetic, Yang-Mills etc.) in our 4D Universe are confined to the three brane. Only gravity can freely propagate in both the brane and bulk space-time, with the gravitational self-couplings not significantly modified. Even if the fifth dimension is uncompactified, standard 4D gravity is reproduced on the brane in the

appropriate limit. Hence this model allows the presence of large, or even infinite non-compact extra dimensions. Our brane is identified to a domain wall in a 5D anti-de Sitter space-time. For a review of the dynamics and geometry of brane universes, see e.g. Maartens & Koyama (2010). In the brane world scenario, the fundamental scale of gravity is not the Planck scale, but another scale which may be at the TeV level. The gravitons propagating through the bulk space give rise to a Kaluza-Klein tower of massive gravitons on the brane. These gravitons couple to the energy-momentum tensor of the standard model fields, and could be produced under the appropriate circumstances as real or virtual particles.

Due to the correction terms coming from the extra dimensions, significant deviations from the standard Einstein theory occur in brane world models at very high energies (Sasaki et al. 2000; Shiromizu et al. 2000; Maeda et al. 2003; Gergely 2003, 2008, 2009). Gravity is largely modified at the electro-weak scale of about 1 TeV. The cosmological and astrophysical implications of the brane world theories have been extensively investigated in the physical literature.

The static vacuum gravitational field equations on the brane depend on the generally unknown Weyl stresses, which can be expressed in terms of two functions, called the dark radiation U and the dark pressure P terms (the projections of the Weyl curvature of the bulk, generating non-local brane stresses) (Dadhich et al. 2000; Germani & Maartens 2001; Gergely 2006; Böhmer & Harko 2007c; Maartens & Koyama 2010). Generally, the vacuum field equations on the brane can be reduced to a system of two ordinary differential equations, which describe all the geometric properties of the vacuum as functions of the dark pressure and dark radiation terms (Harko & Mak 2003). In order to close the system of vacuum field equations on the brane a functional relation between these two quantities is necessary.

The full 5-dimensional Einstein equations have been solved numerically for static, spherically symmetric matter localized on the brane in Wiseman (2002), yielding regular geometries in the bulk with axial symmetry. The same data that specifies stars in 4-dimensional gravity, uniquely constructs a 5-dimensional solution. An upper mass limit is observed for these small stars, and the geometry shows no global pathologies. The intrinsic geometry of large stars, with radius several times the AdS length, is described by four-dimensional General Relativity. The results obtained in Wiseman (2002) show that Randall-Sundrum gravity, with localized brane matter, reproduces relativistic astrophysical solutions, such as neutron stars and massive black holes, in a way which is consistent with observations.

Several classes of spherically symmetric solutions of the static gravitational field equations in the vacuum on the brane have been obtained in Harko & Mak (2003); Mak & Harko (2004); Harko & Mak (2005); Böhmer & Harko (2007c); Gergely (2007); Horváth, Gergely & Hobill (2003). As a possible physical application of these solutions the behavior of the angular velocity v_{tg} of the test particles in stable circular orbits has been considered (Mak & Harko 2004; Harko & Cheng 2006; Böhmer & Harko 2007c; Rahaman et al. 2008). The general form of the solution, together with two constants of integration, uniquely determines the rotational velocity of the particle. In the limit

of large radial distances, and for a particular set of values of the integration constants the angular velocity tends to a constant value. This behavior is typical for massive particles (hydrogen clouds) outside galaxies (Binney & Tremaine 1987), and is usually explained by postulating the existence of the dark matter.

Thus, the rotational galactic curves can be naturally explained in brane world models, without introducing any additional hypothesis (Mak & Harko 2004; Harko & Cheng 2006; Böhmer & Harko 2007c). The galaxy is embedded in a modified, spherically symmetric geometry, generated by the non-zero contribution of the Weyl tensor from the bulk. The extra terms, which can be described in terms of the dark radiation term U and the dark pressure term P , act as a “matter” distribution outside the galaxy. The particles moving in this geometry feel the gravitational effects of U , which can be expressed in terms of an equivalent mass (the dark mass) M_U . The dark mass is linearly increasing with the distance, and proportional to the baryonic mass of the galaxy, $M_U(r) \approx M_B(r/r_0)$ (Mak & Harko 2004; Harko & Cheng 2006; Böhmer & Harko 2007c). The exact galactic metric, the dark radiation and the dark pressure in the flat rotation curves region in the brane world scenario has been obtained in Harko & Cheng (2006).

Similar interpretations of the dark matter as bulk effects have been also considered in Pal et al. (2005) and Pal (2008), where it was also shown that it is possible to model the X-ray profiles of clusters of galaxies, without the need for dark matter.

Hence, a first possible approach to the study of the vacuum brane consists in adopting an explicit equation of state for the dark pressure as a function of the dark radiation. A second method consists in closing the field equations on the brane by imposing the condition of the constancy of the rotational velocity curves for particles in stable orbits.

It is the purpose of the present paper to consider the general behavior of the vacuum gravitational field equations in the brane world model in the region of constant tangential rotational velocity of test particles in stable circular orbits, and to compare the predictions of our model with the existing observational data. Physically, this situation is characteristic for particles gravitating in circular orbits around the galactic center (Binney & Tremaine 1987). As a first step in our study we derive, under the assumption of spherical symmetry, the basic equations describing the structure of the vacuum on the brane, and the equation giving the behavior of the tangential velocity of the test particles as functions of the dark radiation and of the dark pressure.

To obtain the tangential velocity of test particles we analyze the geodesics for a 4D motion by reducing the problem to the motion of a test particle in an effective potential, also containing the effects of the bulk. By assuming that the brane is a fixed point of the bulk, we derive the equation giving the tangential velocity as a function of the g_{tt} component of the metric tensor only. In the region of constant tangential velocities, the general solutions of the gravitational equations can be obtained in an exact analytic form.

To test the viability of the model, and in order to apply it to realistic systems, we compare the theoretical rotation curves with a sample of 18 galaxies that includes both low and high surface brightness galaxies, with measured rotation curves extending in the dark matter dominated region.

From this comparison we obtain the numerical values of the parameters characterizing the equation of state of the Weyl fluid, as well as the parameters giving the behavior of the rotation curves in the brane world models.

Persic et al. (1996) found that spiral rotation curves show that the rotation velocity at any radius depends only on the luminosity. This implies that the galactic rotation curves can be modeled by a Universal Rotation Curve. These curves show a slightly declining velocity in the galactic halo.

The present paper is organized as follows. The field equations in the brane world models, as well as the tangential velocity of test particles in stable circular orbits are presented in Section 2. The structure of the vacuum in the brane world models is analyzed in Section 3. The explicit form of the tangential velocity is obtained, for a specific form of the equation of state of the Weyl fluid, in Section 4. A general theoretical comparison of the tangential velocity relation with the observational constraints is performed in Section 5. In Section 6, by fitting the theoretical predictions of the model with the observational data for a sample of 9 HSB galaxies, the numerical values of the parameters describing the Weyl fluid are determined. We use the same method for the LSB galaxies in Section 7. We discuss and conclude our results in Section 8.

2 FIELD EQUATIONS AND TANGENTIAL VELOCITY OF TEST PARTICLES

In the present Section we present the field equations for static, spherically symmetric vacuum branes, and obtain the velocity of the test particles in stable circular orbits around the galactic center.

2.1 The field equations in the brane world models

We start by considering a five dimensional (5D) space-time (the bulk), with a single four-dimensional (4d) brane, on which ordinary matter is confined, only gravity can probe the extra dimensions. The 4D brane world $({}^{(4)}M, g_{ab})$ is located at a hypersurface $(B(X^A) = 0)$ in the 5d bulk space-time $({}^{(5)}M, {}^{(5)}g_{AB})$, of which coordinates are described by $X^A, A = 0, 1, \dots, 4$. The 4D coordinates on the brane are $x^a, a = 0, 1, 2, 3$. All tensors T_{AB} and vectors V_A satisfy $T_{IJ} = T_{ab}\delta_I^a\delta_J^b$ and $V_A = V_a\delta_A^a$ at the hypersurface.

The action of the system is given by (Sasaki et al. 2000)

$$S = S_{bulk} + S_{brane}, \quad (1)$$

where

$$S_{bulk} = \int_{{}^{(5)}M} \sqrt{-{}^{(5)}g} \left[\frac{1}{2k_5^2} {}^{(5)}R + {}^{(5)}L_m + \Lambda_5 \right] d^5X, \quad (2)$$

and

$$S_{brane} = \int_{{}^{(4)}M} \sqrt{-{}^{(4)}g} \times \left[\frac{1}{k_5^2} K^\pm + L_{brane}(g_{ac}, \psi) + \lambda_b \right] d^4x, \quad (3)$$

where $k_5^2 = 8\pi G_5$ is the 5D gravitational constant, ${}^{(5)}R$ and ${}^{(5)}L_m$ are the 5D scalar curvature and the matter Lagrangian in the bulk, representing non-standard model

fields, $L_{brane}(g_{ab}, \psi)$ is the 4D Lagrangian, which is given by a generic functional of the brane metric g_{ab} and of the matter fields ψ , K^\pm is the trace of the extrinsic curvature on either side of the brane, and Λ_5 and λ_b (the constant brane tension) are the negative vacuum energy densities in the bulk and on the brane, respectively.

The Einstein field equations in the bulk can be obtained as (Sasaki et al. 2000)

$${}^{(5)}G_{IJ} = k_5^2 {}^{(5)}T_{IJ}, \quad (4)$$

where

$${}^{(5)}T_{IJ} \equiv -2 \frac{\delta {}^{(5)}L_m}{\delta {}^{(5)}g^{IJ}} + {}^{(5)}g_{IJ} {}^{(5)}L_m, \quad (5)$$

is the energy-momentum tensor of bulk matter fields. The energy-momentum tensor of the matter localized on the brane, $T_{\mu\nu}$, is defined by

$$T_{ab} \equiv -2 \frac{\delta L_{brane}}{\delta g^{ab}} + g_{ab} L_{brane}. \quad (6)$$

(The minus sign in the above definitions appears because the variation is done with respect to g^{ab} rather than g_{ab} , and there are two terms because the Lagrangian is varied, rather than the Lagrangian density.)

The delta function $\delta(B)$ denotes the localization of brane contribution. In the 5D space-time a brane is a fixed point of the Z_2 symmetry. The basic equations on the brane are obtained by projections onto the brane world. The induced 4D metric is $g_{IJ} = {}^{(5)}g_{IJ} - n_I n_J$, where n_I is the space-like unit vector field normal to the brane hypersurface ${}^{(4)}M$. In the following we assume ${}^{(5)}L_m = 0$.

Assuming a metric of the form $ds^2 = (n_I n_J + g_{IJ}) dx^I dx^J$, with $n_I dx^I = d\chi$ the unit normal to the $\chi = \text{constant}$ hypersurfaces and g_{IJ} the induced metric on $\chi = \text{constant}$ hypersurfaces, the effective 4d gravitational equation on the brane (the effective Einstein equation), takes the form (Sasaki et al. 2000):

$$G_{ab} = k_4^2 T_{ab} + k_5^4 S_{ab} - E_{ab}, \quad (7)$$

where S_{ab} is the local quadratic energy-momentum correction

$$S_{ab} = \frac{1}{12} T T_{ab} - \frac{1}{4} T_a{}^c T_{bc} + \frac{1}{24} g_{ab} (3T^{cd} T_{cd} - T^2), \quad (8)$$

and E_{ab} is the non-local effect from the free bulk gravitational field, the transmitted projection of the bulk Weyl tensor C_{IAJB} , $E_{IJ} = C_{IAJB} n^A n^B$, with the property $E_{IJ} \rightarrow E_{ab} \delta_I^a \delta_J^b$ as $\chi \rightarrow 0$. We have also denoted $k_4^2 = 8\pi G$, with G the usual 4D gravitational constant. In the limit $\lambda_b^{-1} \rightarrow 0$ we recover standard general relativity (Sasaki et al. 2000).

The Einstein equation in the bulk and the Codazzi equation also imply the conservation of the energy-momentum tensor of the matter on the brane, $\nabla_c T_a{}^c = 0$, where ∇_a denotes the brane covariant derivative. Moreover, from the contracted Bianchi identities on the brane it follows that the projected Weyl tensor obeys the constraint $\nabla_c E_a{}^c = k_5^4 \nabla_c S_a{}^c$. Thus the 4-divergence of E_{ab} is constrained by the matter on the brane (Shiromizu et al. 2000).

The generic traceless E_{ab} can be decomposed irreducibly with respect to a chosen 4-velocity field u^a as (Maartens & Koyama 2010)

$$E_{ab} = -k_4^4 \left[U \left(u_a u_b + \frac{1}{3} h_{ab} \right) + P_{ab} + 2Q_{(a} u_{b)} \right], \quad (9)$$

where the induced metric $h_{ab} = g_{ab} + u_a u_b$ projects orthogonal to u^a , the "dark radiation" term $U = -k_4^{-4} E_{ab} u^a u^b$ is a scalar, $Q_a = k_4^{-4} h_a^c E_{cd} u^d$ is a spatial vector, finally $P_{ab} = -k_4^{-4} \left[h_a^c h_b^d - \frac{1}{3} h_{ab} h^{cd} \right] E_{cd}$ is a spatial, symmetric and trace-free tensor.

In the following we neglect the effect of the cosmological constant on the geometry and dynamics of the galactic particles. In the case of the vacuum state we have $\rho = p = 0$, $T_{\mu\nu} \equiv 0$, and consequently $S_{ab} = 0$. Therefore the field equation describing a static brane takes the form

$$R_{ab} = -E_{ab}, \quad (10)$$

with the trace R of the Ricci tensor R_{ab} satisfying the condition $R = R_a{}^a = 0$.

In the vacuum case E_{ab} also satisfies the constraint $\nabla_c E_a{}^c = 0$. In an inertial frame at any point on the brane we have $u^a = \delta_0^a$ and $h_{ab} = \text{diag}(0, 1, 1, 1)$. In a static vacuum $Q_a = 0$ and the constraint for E_{ab} takes the form (Germani & Maartens 2001)

$$\frac{1}{3} D_a U + \frac{4}{3} U A_a + D^b P_{ab} + A^b P_{ab} = 0, \quad (11)$$

where $A_a = u^b \nabla_b u_a$ is the 4-acceleration and D_a denotes the covariant derivative associated to the metric h_{ab} . In the static spherically symmetric case we may chose $A_a = A(r) r_a$ and $P_{ab} = P(r) \left(r_a r_b - \frac{1}{3} h_{ab} \right)$, where $A(r)$ and $P(r)$ (the "dark pressure" although the name dark anisotropic stress might be more appropriate) are some scalar functions of the radial distance r , and r_a is a unit radial vector (Dadhich et al. 2000). Thus the expression (9) simplifies to

$$E_{ab} = -k_4^4 \left[U u_a u_b + \frac{U - P}{3} h_{ab} + P r_a r_b \right]. \quad (12)$$

2.2 The motion of particles in stable circular orbits on the brane

In brane world models test particles are confined to the brane. Mathematically, this means that the equations governing the motion are the standard 4d geodesic equations (Maartens & Koyama 2010). However, the bulk has an effect on the motion of the test particles on the brane via the metric. Since the projected Weyl tensor effectively serves as an additional matter source, the metric is affected by these bulk effects, and so are the geodesic equations. This has to be contrasted with Kaluza-Klein theories, where matter travels on 5d geodesics.

In order to obtain results which are relevant to the galactic dynamics, in the following we will restrict our study to the static and spherically symmetric metric given by

$$ds^2 = -e^{\nu(r)} dt^2 + e^{\lambda(r)} dr^2 + r^2 d\Omega^2, \quad (13)$$

where $d\Omega^2 = d\theta^2 + \sin^2 \theta d\phi^2$.

The Lagrangian \mathcal{L} for a massive test particle traveling on the brane reads

$$\mathcal{L} = \frac{1}{2} \left(-e^\nu \dot{t}^2 + e^\lambda \dot{r}^2 + r^2 \dot{\Omega}^2 \right), \quad (14)$$

where the dot means differentiation with respect to the affine parameter.

Since the metric tensor coefficients do not explicitly depend on t and Ω , the Lagrangian (14) yields the following conserved quantities (generalized momenta):

$$-e^{\nu(r)}\dot{t} = E, \quad r^2\dot{\Omega} = L, \quad (15)$$

where E is related to the total energy of the particle and L to the total angular momentum. With the use of conserved quantities we obtain from Eq. (14) the geodesic equation for massive particles (for which $2\mathcal{L} = -1$ holds) in the form

$$e^{\nu+\lambda}\dot{r}^2 + e^{\nu}\left(1 + \frac{L^2}{r^2}\right) = E^2, \quad (16)$$

The second term of the left-hand side can, in some cases, be interpreted as an effective potential. For instance, for the Schwarzschild space-time, where $e^{\nu+\lambda} = 1$, the kinetic term is position independent. In that case the notion of an effective potential is appropriate. In other cases, even one can still compute the turning points of the kinetic term, however, the effective potential interpretation is lost.

For particles in circular and stable orbits the following conditions must be satisfied: a) $\dot{r} = 0$ (circular motion) b) $\partial V_{eff}/\partial r = 0$ (extreme motion) and c) $\partial^2 V_{eff}/\partial r^2|_{\text{extr}} > 0$ (stable orbit), respectively. Conditions a) and b) immediately give the conserved quantities as

$$E^2 = e^{\nu}\left(1 + \frac{L^2}{r^2}\right), \quad (17)$$

and

$$\frac{L^2}{r^2} = \frac{r\nu'}{2}e^{-\nu}E^2, \quad (18)$$

respectively. Equivalently, these two equations can be rewritten as

$$E^2 = \frac{e^{\nu}}{1 - r\nu'/2}, \quad L^2 = \frac{r^3\nu'/2}{1 - r\nu'/2}. \quad (19)$$

We define the tangential velocity v_{tg} of a test particle on the brane, as measured in terms of the proper time, that is, by an observer located at the given point, as (Landau & Lifshitz 1975)

$$v_{tg}^2 = e^{-\nu}r^2\dot{\Omega}^2t^{-2} = e^{-\nu}\frac{L^2}{r^2}t^{-2}. \quad (20)$$

In the second equality we have employed the second Eq. (15). By eliminating L with Eq. (18) and subsequently E with the first Eq. (15), we obtain the expression of the tangential velocity of a test particle in a stable circular orbit on the brane as (Matos et al. 2000; Nucamendi et al. 2001)

$$v_{tg}^2 = \frac{r\nu'}{2}. \quad (21)$$

Let us emphasize again that the function ν' is obtained by solving the field equations containing the bulk effects as additional matter terms; we consider this in Section 3.

2.3 The gravitational field equations for a static spherically symmetric brane

For the metric given by Eq. (13) the gravitational field equations and the effective energy-momentum tensor conservation equation in the vacuum take the form (Harko & Mak 2003; Mak & Harko 2004)

$$-e^{-\lambda}\left(\frac{1}{r^2} - \frac{\lambda'}{r}\right) + \frac{1}{r^2} = 3\alpha_b U, \quad (22)$$

$$e^{-\lambda}\left(\frac{\nu'}{r} + \frac{1}{r^2}\right) - \frac{1}{r^2} = \alpha_b(U + 2P), \quad (23)$$

$$e^{-\lambda}\frac{1}{2}\left(\nu'' + \frac{\nu'^2}{2} + \frac{\nu' - \lambda'}{r} - \frac{\nu'\lambda'}{2}\right) = \alpha_b(U - P), \quad (24)$$

$$\nu' = -\frac{U' + 2P'}{2U + P} - \frac{6P}{r(2U + P)}, \quad (25)$$

where $' = d/dr$, and we have denoted $\alpha_b = k_4^4/3$. Note that Eq. (25) is a consequence of Eqs. (22), (23) and (24), respectively.

As for the motion of the test particle on the brane we assume that they follow stable circular orbits, with tangential velocities given by Eq. (21). Thus, the rotational velocity of the test body is determined by the metric coefficient $\exp(\nu)$ only.

The field equations (22)–(23) yield the following effective energy density ρ^{eff} , radial pressure P^{eff} and orthogonal pressure P_{\perp}^{eff} , respectively,

$$\rho^{\text{eff}} = 3\alpha_b U, \quad (26)$$

$$P^{\text{eff}} = \alpha_b(U + 2P), \quad (27)$$

$$P_{\perp}^{\text{eff}} = \alpha_b(U - P), \quad (28)$$

which obey $\rho^{\text{eff}} - P^{\text{eff}} - 2P_{\perp}^{\text{eff}} = 0$. This is expected for the ‘radiation’ like source, the projection of the bulk Weyl tensor, which is trace-less, $E_a^a = 0$.

3 STRUCTURE EQUATIONS OF THE VACUUM IN THE BRANE WORLD MODELS

Eq. (22) can immediately be integrated to give

$$e^{-\lambda} = 1 - \frac{C_b}{r} - \frac{GM_U(r)}{r}, \quad (29)$$

where C_b is an arbitrary constant of integration, and we denoted

$$GM_U(r) = 3\alpha_b \int_0^r U(r)r^2 dr. \quad (30)$$

The function M_U is the gravitational mass corresponding to the dark radiation term (the dark mass). For $U = 0$ the metric coefficient given by Eq. (29) must tend to the standard general relativistic Schwarzschild metric coefficient, which gives $C_b = 2GM$, where $M = \text{constant}$ is the baryonic (usual) mass of the gravitating system.

By substituting ν' given by Eq. (25) into Eq. (23) and with the use of Eq. (29) we obtain the following system of differential equations satisfied by the dark radiation term U , the dark pressure P and the dark mass M_U , describing the vacuum gravitational field, exterior to a massive body, in the brane world model (Harko & Mak 2003):

$$\frac{dU}{dr} = -\frac{2v_{tg}^2(2U + P)}{r} - 2\frac{dP}{dr} - \frac{6P}{r}, \quad (31)$$

$$\frac{dM_U}{dr} = \frac{3\alpha_b}{G}r^2U, \quad (32)$$

with the tangential velocity given as

$$v_{tg}^2 = \frac{1}{2}\frac{2GM + GM_U + \alpha_b(U + 2P)r^3}{r\left(1 - \frac{2GM}{r} - \frac{GM_U}{r}\right)}. \quad (33)$$

In order to close the system a supplementary functional relation between one of the unknowns U , P , M_U and v_{tg} is needed. Once this relation is known, Eqs. (31)–(33) give a full description of the geometrical properties and of the motion of the particles on the brane.

The system of equations (31) and (32) can be transformed to an autonomous system of differential equations by means of the transformations

$$\theta = \ln r, \quad q = 1 - e^{-\lambda} = \frac{2GM}{r} + \frac{GM_U}{r}, \quad (34)$$

$$\mu = 3\alpha_b r^2 U, \quad p = 3\alpha_b r^2 P, \quad (35)$$

We shall call μ and p the "reduced" dark radiation and pressure, respectively.

With the use of the new variables given by Eqs. (34), Eqs. (32) and (31) become

$$\frac{dq}{d\theta} = \mu - q, \quad (36)$$

$$\frac{d\mu}{d\theta} = -\frac{(2\mu + p) \left[q + \frac{1}{3}(\mu + 2p) \right]}{1 - q} - 2\frac{dp}{d\theta} + 2\mu - 2p. \quad (37)$$

Eqs. (31) and (32), or, equivalently, (36) and (37) may be called the structure equations of the vacuum on the brane. In order to close this system an "equation of state", relating the reduced dark radiation and the dark pressure terms is needed. Generally, this equation of state is given in the form $P = P(U)$.

In the new variables the tangential velocity of a particle in a stable circular orbit on the brane is given by

$$v_{tg}^2 = \frac{1}{2} \frac{q + \frac{1}{3}(\mu + 2p)}{1 - q}. \quad (38)$$

By using the expression of the tangential velocity, Eq. (37) can be rewritten as

$$\frac{d}{d\theta} (\mu + 2p) = -2(2\mu + p) v_{tg}^2 + 2\mu - 2p. \quad (39)$$

Eqs. (38) and (39) allow the easy check of the physical consistency of some simple equations of state for the dark pressure. The equation of state $\mu + 2p = 0$ immediately gives $v_{tg}^2 = 1$ and $q = 2/3$, respectively, implying that all test particles in stable circular motion on the brane move at the speed of light. This result contradicts the assumption that the test particles are time-like, as well as the observations on galactic scale. Therefore the equation of state $\mu + 2p = 0$ is not consistent with the rotation curves. The equation of state $2\mu + p = 0$ gives $\mu = \mu_0/r^2$, where $\mu_0 = \text{constant}$ is an arbitrary integration constant, $U = \mu_0/3\alpha_b r^4$ and $GM_U = -\mu_0/3r^3$, respectively. In the limit of large r , the tangential velocity v_{tg}^2 tends to zero, $v_{tg} \rightarrow 0$. Therefore, this model seems also to be ruled out by observations. The case $\mu = p$ gives $\mu(\theta) = \mu_0 \exp \left[-2 \int v_{tg}^2(\theta) d\theta \right]$, $\mu_0 = \text{constant}$, and $q(\theta) = (2v_{tg}^2 - \mu) / (1 + 2v_{tg}^2)$.

4 TANGENTIAL VELOCITY FOR GALAXIES FOR A LINEAR EQUATION OF STATE OF THE WEYL FLUID

4.1 Linear equation of state for the Weyl fluid

In order to close the system of equations Eqs. (36) and (37), we need to specify the equation of state relating the dark

acceleration	expansion	shear	vorticity
A	0	0	0

Table 1. Kinematical scalars of the congruence u^b in the 3+1 decomposition of $\nabla_a u_b$.

acceleration	expansion	shear	vorticity
0	$\tilde{\Theta}$	0	0

Table 2. Kinematical scalars of the congruence r^b in the 2+1 decomposition of $D_a r_b$.

pressure to the dark radiation. In the full 5-dimensional approach of Wiseman (2002) the Einstein field equations were solved numerically for static, spherically symmetric matter localized on the brane, yielding regular geometries in a bulk with axial symmetry. For this a density profile, taken as a deformed top hat function, was imposed.

An alternative approach for closing the system of field equations can be obtained from the 3+1+1 covariant approach in brane worlds, developed in Keresztes & Gergely (2010a,b). First, we impose: i) cosmological vacuum in 5-dimensional spacetime, ii) the brane embedding is symmetrical, iii) fine-tuning on the brane (the brane cosmological constant vanishes), iv) no matter on the brane, v) the brane is static and spherical symmetric, with metric given by Eq. (13). The set of gravito-electro-magnetic quantities in the 3+1+1 covariant approach is presented in Appendix I. Due to assumptions ii) and iv) the Lanczos equations impose that the tensorial and vectorial projections of the extrinsic brane curvature along the brane normal n^A vanish: $\hat{\sigma}_{ab} = 0 = \hat{K}_a$. Therefore $\mathcal{E}_{ab} = \tilde{E}_{ab} - k_4^4 P_{ab}/2$ and $\mathcal{H}_{ab} = \tilde{H}_{ab}$, respectively.

From the above assumptions we also find that the only nonzero kinematical quantity related to the normal u^a of the $t = \text{const.}$ hypersurfaces is its acceleration $A_a = u^b D_b u_a$ (here D_a is the covariant derivative on the brane). The kinematical quantities of the vector congruences u^a and r^a are enlisted in Tables 1 and 2.

Due to the spherical symmetry, assumption v), it is convenient to decompose the brane spacetime into a 2+1+1 form. Then the gravito-electro-magnetic quantities appearing in the brane equations further reduce to $H_{ab} = 0$, $\tilde{E}_{ab} = \tilde{E}(r)(r_a r_b - h_{ab}/3)$, $k_4^4 U(r)$, $Q_a = 0$ and $k_4^4 P_{ab} = k_4^4 P(r)(r_a r_b - h_{ab}/3)$, respectively, while $A_a = A(r)r_a$. Therefore under the assumption of spherical symmetry the Weyl fluid is characterized by the set $U(r)$, $P(r)$; the electric part of 4-dimensional Weyl tensor by $\tilde{E}(r)$; and the acceleration of the time-like normal to the 3-space by $A(r)$.

We also introduce the covariant derivative ${}^{(3)}D_a$ associated with the 3-metric h_{ab} and the expansion $\tilde{\Theta}(r)$ of the radial geodesics in the local three-dimensional space (obeying $r^a {}^{(3)}D_a r_b = 0$) by the relation ${}^{(3)}D^a r_a = \tilde{\Theta}(r)$. The 4 independent field equations for the variables U , P , \tilde{E} , A , and $\tilde{\Theta}$, arising in the 2+1+1 brane formalism are given in Appendix II. There are two algebraic equations [Eqs. (108) and (112)] determining U and P as function of \tilde{E} , A , and $\tilde{\Theta}$:

$$k_4^4 U = \tilde{\Theta} \left(A - \frac{\tilde{\Theta}}{4} \right) + \frac{4\tilde{E}}{3} + \frac{1}{r^2}, \quad (40)$$

$$k_4^4 P = \tilde{\Theta} \left(A + \frac{\tilde{\Theta}}{2} \right) - \frac{2\tilde{E}}{3} - \frac{2}{r^2}, \quad (41)$$

and two first order non-linear ordinary differential equations [Eqs. (114) and (115)] for the variables A , $\tilde{\Theta}$ (also containing \tilde{E}):

$$\frac{r\tilde{\Theta}}{2}\tilde{\Theta}' + \frac{\tilde{\Theta}^2}{2} + \frac{4\tilde{E}}{3} + A\tilde{\Theta} = 0, \quad (42)$$

$$\frac{r\tilde{\Theta}}{2}A' + A^2 + \frac{\tilde{\Theta}^2}{4} - \frac{4\tilde{E}}{3} - \frac{1}{r^2} = 0. \quad (43)$$

The last two equations contain only quantities defined and determined by the brane dynamics. In order to obtain a special solution of the system (42)-(43), we need a third relation between the brane kinematic quantities A , $\tilde{\Theta}$ and electric Weyl brane curvature \tilde{E} . In order to establish this, first we remark, that in the Schwarzschild case these quantities obey

$$\frac{2\tilde{E}}{3} + \tilde{\Theta}A = \tilde{\Theta} \left(\frac{\tilde{\Theta}}{4} + A \right) - \frac{1}{r^2} = 0. \quad (44)$$

By virtue of these the two Eqs. (42)-(43) are found to coincide, thus A , $\tilde{\Theta}$ and \tilde{E} are still defined by a set of three equations. For a spherically symmetric solution on the brane we allow for a slightly modified identity as compared to the first Eq. (44):

$$\frac{2\tilde{E}}{3} + \tilde{\Theta}A = \mathcal{A}\tilde{\Theta} \left(\frac{\tilde{\Theta}}{4} + A \right) - \frac{\mathcal{B}}{r^2}, \quad (45)$$

with \mathcal{A} and \mathcal{B} two constants, both reducing to 1 in Schwarzschild case. By employing Eqs. (40), (41), this equation can be rewritten as a simple equation of state for the Weyl fluid:

$$P = (a - 2)U - \frac{\mathcal{B}}{k_4^4 r^2}. \quad (46)$$

Here we have introduced the new constants a, \mathcal{B} by redefining $\mathcal{A} = a/(2a - 3)$, $\mathcal{B} = (a - \mathcal{B})/(2a - 3)$. We also remark that in the variables given by Eq. (34) the equation (46) takes the simple linear form

$$p(\mu) = (a - 2)\mu - \mathcal{B}. \quad (47)$$

The system (42)-(43) and (45), being a first order ordinary system of differential equations, determines the variables A , $\tilde{\Theta}$ and \tilde{E} . Their existence is assured by the Cauchy-Peano theorem. When rewritten in metric variables, the solution valid in the region where rotation curve data is available will be obtained in the following subsection.

One can be rightfully worried about the compatibility of Eq. (46) with the full 5-dimensional gravitational dynamics, however this is but a boundary condition imposed on the brane at some arbitrary time. Then the static character of the problem assures that it is preserved by the dynamics throughout the temporal evolution.

Looking to this problem from a mathematical point of view, for the system of first order differential equations describing the the extra dimensional evolution Keresztes & Gergely (2010a), the choice of the Weyl fluid variables represents an "initial condition" in any suitable off-brane parameter (for example, the one associated with the

integral curves of the vector field n^A). Such "initial values" could be chosen arbitrarily except when there is a constraint to be obeyed on the "initial surface". This surface being the brane, the condition to be obeyed is the constraint equation for the Weyl fluid, Eq. (11). As shown in Appendix II, on a static and spherically symmetric brane Eq. (11) simplifies to Eq. (115). It is not very difficult to see, that this equation follows from the system (40)-(43). Therefore the constraint for the Weyl fluid is trivially satisfied in the static and spherically symmetric case and the particular choice of "initial conditions" (45) is allowed, as would be any other choice. The advantage of choosing Eq. (45) is, however, that it leads to the simple linear equation of state in the reduced Weyl variables p and μ . We will see that the confrontation of the model with galactic rotation curve data supports the choice (45) from a physical point of view either.

4.2 The metric and tangential velocity on the brane

The dark radiation and the dark pressure can be obtained as a functions of the tangential velocity in a closed analytical form for the equation of state given by Eq. (47). The reduced dark radiation can be obtained as

$$\begin{aligned} \mu(\theta) &= \theta^{2(3-a)/(2a-3)} \exp \left[-\frac{2a}{2a-3} \int v_{tg}^2(\theta) d\theta \right] \times \\ &\left\{ C_0 - \frac{3\mathcal{B}}{2a-3} \int [1 + v_{tg}^2(\theta)] \theta^{-2(3-a)/(2a-3)} \times \right. \\ &\left. \exp \left[\frac{2a}{2a-3} \int v_{tg}^2(\theta) d\theta \right] \right\}, \quad (48) \end{aligned}$$

where C_0 is an arbitrary integration constant. Hence, if the velocity profile of a test particle in stable circular motion is known, one can obtain all the relevant physical parameters for a static spherically symmetric system on the brane.

By using the linear equation of state of the dark pressure Eq. (37) takes the form

$$(2a - 3) \frac{d\mu}{d\theta} = -\frac{(a\mu - \mathcal{B}) [q + (2a - 3)\mu/3 - 2\mathcal{B}/3]}{1 - q} + 2(3 - a)\mu + 2\mathcal{B}, \quad (49)$$

where we have neglected the possible effect of the cosmological constant on the structure of the cluster. Due to the mathematical structure of Eq. (49) there are two cases that can be considered separately, $a = 3/2$, and $a \neq 3/2$, respectively.

For a galactic dark matter halo with mass of the order of $M = 10^{12} M_\odot$ and radius $R = 100$ kpc, the quantity $2GM/R$ is of the order of 9.6×10^{-7} , which is much smaller than one. Since observations show that inside the galaxy the mass is a linearly increasing function of the radius r , the value of this ratio is roughly the same at all points in the galaxy. Therefore from its definition it follows that generally $q \ll 1$, and $1 - q \approx 1$. Moreover, the quantities q^2 and $qdq/d\theta$ are also very small as compared to q . Eq. (36) gives $\mu = q + dq/d\theta$, $d\mu/d\theta = dq/d\theta + d^2q/d\theta^2$.

4.2.1 The case $a \neq 3/2$

Hence, by neglecting the second order terms and assuming $a \neq 3/2$, we obtain for q the following differential equation:

$$\frac{d^2q}{d\theta^2} + m\frac{dq}{d\theta} - nq = b, \quad (50)$$

where we have denoted

$$m = 1 - \frac{B}{3} - \frac{2}{3} \frac{a(B-3)+9}{2a-3}, a \neq \frac{3}{2}, \quad (51)$$

$$n = \frac{2}{3} \frac{a(2B-3)+9}{2a-3}, a \neq \frac{3}{2}, \quad (52)$$

and

$$b = \frac{2}{3} \frac{B(B-3)}{3-2a}, a \neq \frac{3}{2}, \quad (53)$$

respectively. The general solution of Eq. (50) is given by

$$q(\theta) = v_0 + C_1 e^{l_1\theta} + C_2 e^{l_2\theta}, a \neq \frac{3}{2}, \quad (54)$$

where C_1 and C_2 are arbitrary constants of integration, and we denoted

$$v_0 = -\frac{b}{n} = \frac{B(B-3)}{a(2B-3)+9}, \quad (55)$$

and

$$l_{1,2} = \frac{-m \pm \sqrt{m^2 + 4n}}{2}, \quad (56)$$

respectively. The reduced dark radiation term is given by

$$\mu(\theta) = v_0 + C_1(1+l_1)e^{l_1\theta} + C_2(1+l_2)e^{l_2\theta}. \quad (57)$$

The tangential velocity of a test particle in the "dark matter" dominated region is given by

$$v_{ig}^2 \approx \frac{1}{2} \left[q + \frac{1}{3}(\mu + 2p) \right] \approx \frac{1}{2} \left[q + \frac{(2a-3)\mu - 2B}{3} \right], \quad (58)$$

or

$$v_{ig}^2(\theta) \approx v_{ig\infty}^2 + \gamma e^{l_1\theta} + \eta e^{l_2\theta}, \quad (59)$$

where we have denoted

$$v_{ig\infty}^2 = \frac{1}{3}(av_0 - B), \quad (60)$$

$$\gamma = \frac{1}{2} \left[\frac{2a-3}{3}(1+l_1) + 1 \right] C_1, \quad (61)$$

$$\eta = \frac{1}{2} \left[\frac{2a-3}{3}(1+l_2) + 1 \right] C_2. \quad (62)$$

In the initial radial coordinate r the tangential velocity can be expressed as

$$v_{ig}^2(r) \approx v_{ig\infty}^2 + \gamma r^{l_1} + \eta r^{l_2}. \quad (63)$$

In order to have an asymptotically constant $v_{ig}^2(r)$, both l_1 and l_2 should be negative numbers, $l_1 < 0$ and $l_2 < 0$, respectively. This can be achieved if $m > 0$, $n < 0$ hold simultaneously.

In the original radial variable r we obtain for the dark radiation and the mass distribution inside the cluster the expressions

$$3\alpha_b U(r) = \frac{v_0}{r^2} + C_1(1+l_1)r^{l_1-2} + C_2(1+l_2)r^{l_2-2}, \quad (64)$$

and

$$GM_U(r) = r(v_0 + C_1 r^{l_1} + C_2 r^{l_2}) - 2GM, \quad (65)$$

respectively, where we have neglected the possible effect of the cosmological constant. The first term in the mass profile

of the dark mass given by Eq. (65) is linearly increasing with r , thus having a similar behavior to the dark matter outside galaxies. The second and third terms in Eq. (65) are either constants (for $l_{1,2} = -1$) or they decrease with increasing r , as $l_{1,2} < 0$.

Finally, the metric coefficient ν can be calculated from the equation

$$\frac{d\nu(\theta)}{d\theta} = q(\theta) + \frac{2a-3}{3}\mu(\theta) - \frac{2B}{3}, \quad (66)$$

giving

$$e^{\nu(r)} = C_\nu r^{2v_{ig\infty}^2} \times \exp \left[C_1 \frac{3 + (2a-3)(1+l_1)}{3l_1} r^{l_1} + C_2 \frac{3 + (2a-3)(1+l_2)}{3l_2} r^{l_2} \right], \quad (67)$$

where C_ν is an arbitrary integration constant. In the limit of large distances $e^{\nu(r)}$ behaves like $e^{\nu(r)} \approx C_\nu r^{2v_{ig\infty}^2}$. Inside the galaxy we can approximate $e^{-\lambda} \approx 1 - C/r - GM_U(r)/r$.

A few comments are in order. First, in the particular case $B = 0$, we have $v_0 \equiv 0$, and in consequence the obtained mass profile is not consistent in general with observations, as for such an equation of state the dark radiation usually cannot play the role of the dark matter (it has no r^{-1} term). For example in the case $a = 4$, corresponding to an equation of state $P = 2U$, the dark mass is given by $GM_U(r) = C_1/r^{1.97} + C_2/r^{0.82} - C_b$.

Secondly, the effective, geometry induced mass must satisfy the condition $M_U \geq 0$. Therefore the solution obtained in the present Section is valid only for values of the coordinate radius r so that $v_0 r + C_1 r^{l_1+1} + C_2 r^{l_2+1} - C \geq 0$. In the limit of small r , taking into account that $l_1 < 0$ and $l_2 < 0$, and by assuming that the coefficient of the dominant term (either v_0 , C_1 or C_2) is positive, the dark mass diverges at the center of the cluster, $\lim_{r \rightarrow 0} M_U(r) = \infty$. Otherwise there is a point r_0 , where $M_U(r_0) \approx 0$ and $M_U(r) < 0$, for $r < r_0$. In this case the solution has physically acceptable properties only in the region $r \geq r_0$.

5 FURTHER SIMPLIFICATION FROM OBSERVATIONAL CONSTRAINTS

In Section 4 the assumption $q \ll 1$ was made in order to derive the analytical solution. As it can be seen from its definition, the quantity q is basically a post-Newtonian parameter and as such the assumption is justified when studying galactic rotation curves. Further, as we are studying bounded motions in the galaxy, due to the virial theorem v_{ig}^2 should be of the same order. Eq. (38), and the remark preceding Subsection IV.A, stating $\mu \ll 1$, together imply $p \ll 1$. Then, from the definition of p , Eq. (47) the condition $B \ll a - 2$ stems out. In other words, B/a should be of the same order of magnitude as μ and q , respectively.

In what follows, we will use the above remark for simplifying the generic results established for $a \neq 3/2$ in the previous Section. For the parameters m , n we obtain

$$m \approx \frac{4a-9}{2a-3}, \quad n \approx -2 \frac{a-3}{2a-3}, \quad (68)$$

which give

$$l_1 \approx -1, \quad l_2 \approx -1 + \frac{3}{2a-3}. \quad (69)$$

In order $l_2 < 0$ to hold (or equivalently $m > 0$ and $n < 0$), the constant a must take values in the range $a \in (-\infty, 3/2) \cup (3, \infty)$.

With these values of $l_{1,2}$ the constants $C_{1,2}$ simplify to $\gamma \approx C_1/2$ and $\eta \approx C_2$. We also get

$$v_0 = \frac{B(B-3)/a}{2B-3+9/a} \approx \frac{B}{a-3}, \quad (70)$$

for any a in the allowed domain. The rotational velocity at infinity then becomes

$$v_{tg\infty}^2 = \frac{a}{3} \left(v_0 - \frac{B}{a} \right) \approx \frac{B}{a-3}, \quad (71)$$

Obviously $v_{tg\infty}^2 \geq 0$, therefore *either* $a < 3/2$ and $B \leq 0$ or $a > 3$ and $B > 0$.

The metric functions approximate as

$$3\alpha_b U(r) \approx \frac{v_0}{r^2} + \frac{3C_2}{2a-3} r^{-3(1-\frac{1}{2a-3})}, \quad (72)$$

$$GM_U(r) \approx v_0 r + C_1 + C_2 r^{\frac{3}{2a-3}} - 2GM, \quad (73)$$

$$e^{\nu(r)} \approx C_\nu r^{2v_{tg\infty}^2} \exp \left[-C_1 r^{-1} - C_2 \frac{2a-3}{a-3} r^{-1+\frac{3}{2a-3}} \right], \quad (74)$$

and for a generic r the rotational velocity can be written as

$$v_{tg}^2(r) \approx \frac{B}{a-3} + \frac{C_1}{2} r^{-1} + C_2 r^{-1+\frac{3}{2a-3}}. \quad (75)$$

By defining $\alpha = 3/(2a-3) = l_2+1$ and $\beta = B/(a-3)$, respectively; then re-introducing the velocity of light c for dimensional reasons; by replacing C_1 with a mass type constant $M+M_0 = C_1/2Gc^2$, and also by rescaling the constant C_2 as $C_2 = Cc^2 r_b^{1-\alpha}$, we obtain

$$\left(\frac{v_{tg}(r)}{c} \right)^2 \approx \frac{G(M_b^{tot} + M_0^{tot})}{c^2 r} + \beta + C \left(\frac{r_b}{r} \right)^{1-\alpha}, \quad r > r^*. \quad (76)$$

Here we have changed the notations (M, M_0) to (M_b^{tot}, M_0^{tot}) for reasons to be explained in what follows. This solution is valid for any $r > r^*$, where r^* represents the radius beyond which the baryonic matter does not extend. We interpret the constant M_b^{tot} as the total baryonic mass inside radius r^* , while M_0^{tot} is a universal constant due to the brane fluid. Thus the Weyl fluid is characterized by three universal dimensionless constants α , β , C and a mass-type constant M_0^{tot} . Also an arbitrary scaling constant r_b was introduced in order to have C dimensionless.

Due to the constraints established for the Weyl fluid parameters a and B , the newly introduced constants α , β obey *either* $\alpha < 0$ or $0 < \alpha < 1$ (the value $\alpha = 0$ is excluded, as it would correspond to the unphysical values $a \rightarrow \pm\infty$) *in both cases* β being a small positive number $0 < \beta \ll 1$ (with the exception of $a \approx 3$, translating to $\alpha \approx 1$, when β can be an arbitrary positive number).

6 HIGH SURFACE BRIGHTNESS GALAXIES

6.1 The baryonic sector: the bulge-disk decomposition

We model the distribution of baryonic mass in High Surface Brightness galaxies as a sum of disk and bulge components

with constant, but distinct mass-to-light ratios. We estimate the bulge parameters from a Sérsic $r^{1/n}$ bulge model and the disk parameters from an exponential disk model, both fitted to the optical I-band galaxy light profiles.

The surface brightness (specific intensity) of the spheroidal bulge component of each galaxy is given by a generalized Sérsic function (Sérsic 1968):

$$I_b(r) = I_{0,b} \exp \left[- \left(\frac{r}{r_0} \right)^{1/n} \right], \quad (77)$$

where $I_{0,b}$ is the central surface brightness of the bulge, r_0 is its characteristic radius and n is the shape parameter of the magnitude-radius curve. As a rule, early-type spiral galaxy bulges have $n > 1$, while late-type spiral galaxy bulges are characterized by $n < 1$. The radius of the bulge r_b is defined by the condition of the surface brightness being equal to $\mu_0 = 2,64 \times 10^{-4}$ mJy · arcsec⁻² in the I-band images.

In a spiral galaxy, the radial surface brightness profile of the disk exponentially decreases with the radius (Freeman 1970)

$$I_d(r) = I_{0,d} \exp \left(- \frac{r}{h} \right), \quad (78)$$

where $I_{0,d}$ is the disk central surface brightness and h is a characteristic disk length scale. In order to measure the light and mass distribution in the disk, the model image of the bulge is subtracted from the original I-band image. All remaining light in these images is then assumed to originate from the disk component.

The (bolometric) luminosity of any of the galaxy components is an integral over surface, solid angle and frequency of I_b and I_d , respectively. The respective mass over luminosity is the mass-to-light ratio - for the Sun $\gamma_\odot = 5133$ kg W⁻¹. The mass-to-light ratios of the bulge and disk σ and τ_b will be given in units of γ_\odot (solar units). We will also give the masses in units of the solar mass $M_\odot = 1.98892 \times 10^{30}$ kg. Assuming that the mass distribution of a spiral galaxy follows the de-projected surface brightness distribution (Kannapan & Gawiser (2007); Portinari et al. (2004) (corrected with respect to the inclination, cf. (Palunas & Williams 2000), with constant mass-to-light ratios σ and τ_b the bulge and disk masses within the radius r are

$$M_b(r) = \sigma \frac{\mathcal{N}(D)}{F_\odot} 2\pi \int_0^r I_b(r) r dr, \quad (79)$$

$$M_d(r) = \tau_b \frac{\mathcal{N}(D)}{F_\odot} 2\pi \int_0^r I_d(r) r dr, \quad (80)$$

where $F_\odot(D)$ is the apparent flux density of the Sun at a distance D Mpc, $F_\odot(D) = 2.635 \times 10^{6-0.4f_\odot}$ mJy, with $f_\odot = 4.08 + 5 \lg(D/1 \text{ Mpc}) + 25$ mag, and

$$\mathcal{N}(D) = 4.4684 \times 10^{-35} D^{-2} \text{ m}^{-2} \text{ arcsec}^2. \quad (81)$$

The baryonic matter at any r is given by

$$M_{baryonic}(r) = M_b(r) + M_d(r). \quad (82)$$

In Palunas & Williams (2000) a maximum disk mass model was presented, and the bulge-disk decompositions was performed for a sample of 74 high surface brightness spiral

galaxies, for which the I-band surface brightness profiles and H_α velocity profiles were also given. From this set we have left out those galaxies, which either have bars or rings, which would both contradict the assumption of spherical symmetry. In addition we have left out the galaxies for which the above baryonic model can not be applied, since they have non-vanishing bulge surface brightness values, but vanishing bulge mass (Palunas & Williams 2000). And finally we have also omitted the galaxies where the observed data sequence exhibits a wavy pattern instead of a plateau, suggesting a disk structure strongly contradicting our assumption for rotational symmetry about the galaxy center. Such patterns are illustrated in Fig. 1. As a result of this selection process we end up with 9 galaxies. Their rotation curves are represented on Fig. 2.

As for the bulge parameters of the 9 selected galaxies, we have derived the best fitting values of $I_{0,b}$, n , r_0 , r_b , $I_{0,d}$, and h from the photometric data as well as the mass-to-light ratio of each component σ and τ_b by fitting Eq. (82) to the data on rotation curves represented on Fig. 1 of Palunas & Williams (2000). These are all collected in Table 3.

6.2 Combined baryonic and Weyl model

We assume that within the bulge radius r_b the contribution of the Weyl-fluid can be neglected and the part of the observed rotation curves lying below r_b could be explained with baryonic matter alone. Outside this radius we switch on the Weyl-fluid and we take into account the exponential disk as a perturbation that does not affect the geometry. We add, however, its contribution to the rotation velocity,

$$v_{tg}^2(r) = \frac{G[M_b(r) + M_d(r)]}{r} + c^2 \left[\beta + C \left(\frac{r_b}{r} \right)^{1-\alpha} \right] H_k(r_b), \quad (83)$$

where $H_k(r_b)$ is some function smoothly approaching the Heaviside step function:

$$H(r_b) = \lim_{k \rightarrow \infty} H_k(r_b) = \begin{cases} 0, & r < r_b \\ 1, & r \geq r_b \end{cases}. \quad (84)$$

The parameter M_0^{tot} of the Weyl fluid in Eq. (76) represents the contribution of the equivalent Weyl mass from the spheres within a given radius. As such a contribution is taken care by the first terms of Eq. (83), we have chosen $M_0^{tot} = 0$.

For $H_k(r_b)$ we choose the logistic function:

$$H_k(r_b) = \frac{1}{1 + \exp(-2k(r - r_b))}. \quad (85)$$

The value of k gives the sharpness of the transition. We determine the parameter k by imposing the conditions $H_k(0.95r_b) = 0.001$, which also implies $H_k(1.05r_b) = 0.999$ and $H_k(r_b) = 0.5$ and its values are given in Table 3 for each of the 9 selected galaxies (Palunas & Williams 2000).

The baryonic parameters τ_b , σ and the Weyl parameter α have to be determined by a χ^2 -minimization fitting of Eqs. (77) - (85), with the rotation curve data for each individual galaxy. The parameter β of Weyl sector gives the asymptotic rotation velocity. We identify β with the average of the points of the rotation curves for $r > r_b$ (these are on the plateau).

At the end of this subsection we prove that the "truncation" of the Weyl fluid at r_b does not induce any distributional source layer at r_b , thus it is consistent with the junction conditions across the sphere with radius r_b . For this we first remark that at a formal level the truncation can be imposed in all equations by the replacements $\beta \rightarrow \beta H_k(r_b)$. By also keeping in mind that $C = C_2 c^{-2} r_b^{\alpha-1} = -\beta$ was chosen, Eq. (72) shows that U smooths to zero with $H_k(r_b)$ across r_b . The equation of state (47) and $B = (3\beta/2)(1/\alpha - 1)$ then guarantees that P has the same property. As both inside and outside r_b we have the same spherically symmetric metric and the energy-momentum tensor changes smoothly across r_b , there is no discontinuity in either the metric or its first derivative, therefore the even stronger Lichnerowicz continuity conditions are obeyed. The Israel-Lanczos-Darmois junction conditions of the continuity of induced metric and extrinsic curvature thus follow. Our approach is different from that used by Wiseman (2002), in which a given density profile is considered, together with the condition of the isotropy on the brane. Therefore, while in Wiseman (2002) the matching conditions impose these requirements as boundary conditions, in our approach the matching conditions are automatically satisfied.

6.3 HSB galaxy rotation curves

Despite of the differences in the surface brightness profiles and rotation curves for the chosen HSB galaxies, the combined baryonic+Weyl model Eq. (83) fits well the sample.

A restriction on the parameter space emerges as $\beta = -C$ from the condition that the Weyl contribution to $v_{tg}^2(r)$ vanishes at r_b (by switching on the Weyl fluid at $r = r_b$). Therefore Eq. (83) simplifies to

$$v_{tg}^2(r) = \frac{G[M_b(r) + M_d(r)]}{r} + c^2 \beta \left[1 - \left(\frac{r_b}{r} \right)^{1-\alpha} \right] H_k(r_b). \quad (86)$$

The rotation curves themselves together with the data are shown on Fig. 2.

7 LOW SURFACE BRIGHTNESS GALAXIES

7.1 LSB galaxy rotation curves

A typical LSB galaxy resembles a normal late-type spiral, usually with some ill-defined spiral arms. They usually have HI masses of a few times $10^9 M_\odot$. Thuan et al. (1987) and Bothun et al. (1993) have found that, although LSB galaxies follow the spatial distribution of HSB galaxies, they tend to be more isolated from their nearest neighbors than HSB galaxies. LSB galaxies can be distinguished from the galaxies defining the Hubble sequence by their low surface brightness, rather than small size (LSB galaxies are not necessarily dwarfs). The central surface brightness of LSB galaxies is much lower than $\mu_B(0) = 21.65 \pm 0.3 \text{ mag-arcsec}^2$ - the typical B-band value for HSB galaxies, established by the Freeman law (Freeman (1970); ?).

The mass density distribution of LSB galaxies at small radii is dominated by a nearly constant density core with a total mass M_0 , and a radius r_c of only a few kpc, as

Galaxy	D	$I_{0,b}$	n	r_0	r_b	$I_{0,d}$	h	k	σ	τ_b	α	β	χ^2_{\min}
	Mpc	mJy/arcsec ²	kpc	kpc	kpc	mJy/arcsec ²	kpc	kpc ⁻¹	\odot	\odot			
ESO215G39	61.29	0.1171	0.6609	0.78	2.58	0.0339	4.11	26.28	0.04	2.1	0.67	2.37×10^{-7}	28.29
ESO322G76	64.28	0.2383	0.8344	0.91	4.50	0.0251	5.28	15.35	0.47	3.28	0.76	3.21×10^{-7}	38.69
ESO322G77	38.19	0.1949	0.7552	0.33	1.37	0.0744	2.20	50.32	1.27	2.7	0.57	3.92×10^{-7}	10.15
ESO323G25	59.76	0.1113	0.4626	0.43	0.99	0.0825	3.47	34.58	2.96	1.85	0.69	5.25×10^{-7}	34.77
ESO383G02	85.40	0.6479	0.7408	0.42	1.94	0.5118	3.82	17.79	0.47	0.22	0.70	3.72×10^{-7}	21.55
ESO445G19	66.05	0.1702	0.6133	0.57	1.79	0.0478	4.27	38.59	1	1.39	0.46	3.64×10^{-7}	29.26
ESO446G01	98.34	0.2093	0.8427	1.28	6.33	0.0357	5.25	10.90	0.93	2.82	0.54	4.64×10^{-7}	43.35
ESO509G80	92.86	0.2090	0.7621	1.10	4.69	0.0176	11.03	14.75	0.61	5.50	0.87	6.3×10^{-7}	25.71
ESO569G17	57.77	0.2452	0.4985	0.45	1.18	0.1348	2.06	58.74	0.06	1.4	0.65	3.18×10^{-7}	7.24

Table 3. The baryonic parameters (D , $I_{0,b}$, n , r_0 , r_b , $I_{0,d}$, h , k) of the 9 HSB galaxy sample. The additional baryonic parameters σ , τ_b and the Weyl parameter α are determined by χ^2 fitting. The best fit parameters ($\sigma = M_b/L_b$, $\tau_b = M_d/L_d$, α) and the minimum value of the χ^2 statistic χ^2_{\min} are also given. All χ^2_{\min} are within 1σ .

Galaxy	k	M_0	r_c	α	β	χ^2_{\min}
	kpc ⁻¹	\odot	kpc			
DDO 189	57.5	4.05×10^8	1.25	0.3	6.43×10^{-8}	0.742
NGC 2366	46.0	1.05×10^9	1.47	0.8	1.12×10^{-7}	2.538
NGC 3274	138.1	4.38×10^8	0.69	-0.4	6.73×10^{-8}	18.099
NGC 4395	30.0	2.37×10^8	0.71	0.9	3.43×10^{-7}	27.98
NGC 4455	99.7	2.26×10^8	1.03	0.9	2.72×10^{-7}	7.129
NGC 5023	86.3	2.69×10^8	0.74	0.9	4.53×10^{-7}	10.614
UGC 10310	36.4	1.28×10^9	2.6	0.4	1.12×10^{-7}	0.729
UGC 1230	15.3	3.87×10^9	3.22	-1.7	1.12×10^{-7}	0.539
UGC 3137	34.5	5.32×10^9	3.87	-0.5	1.23×10^{-7}	4.877

Table 4. The best fit parameters of the 9 LSB galaxy sample (M_0 , r_c , α , β). The minimum values of the χ^2 statistic χ^2_{\min} are also given. All χ^2_{\min} are within 1σ .

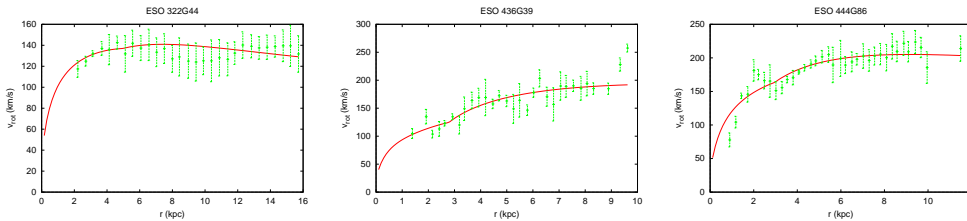


Figure 1. Three examples of galaxies omitted due to the wavy pattern data sequence. The best fits of our model are also shown, all outside the 1σ confidence level.

Galaxy	M_{Weyl}	$M_{simulation}$
	$10^{12} M_{\odot}$	$10^{12} M_{\odot}$
ESO215G39	1.27	1.89
ESO322G76	2.43	8.53
ESO322G77	2.19	1.487
ESO323G25	3.75	3.76
ESO383G02	2.35	3.12
ESO445G19	2.33	1.97
ESO446G01	4.69	9.7
ESO509G80	10.7	205
ESO569G17	1.55	1.17

Table 5. The calculated halo masses for the investigated sample of HSB galaxies.

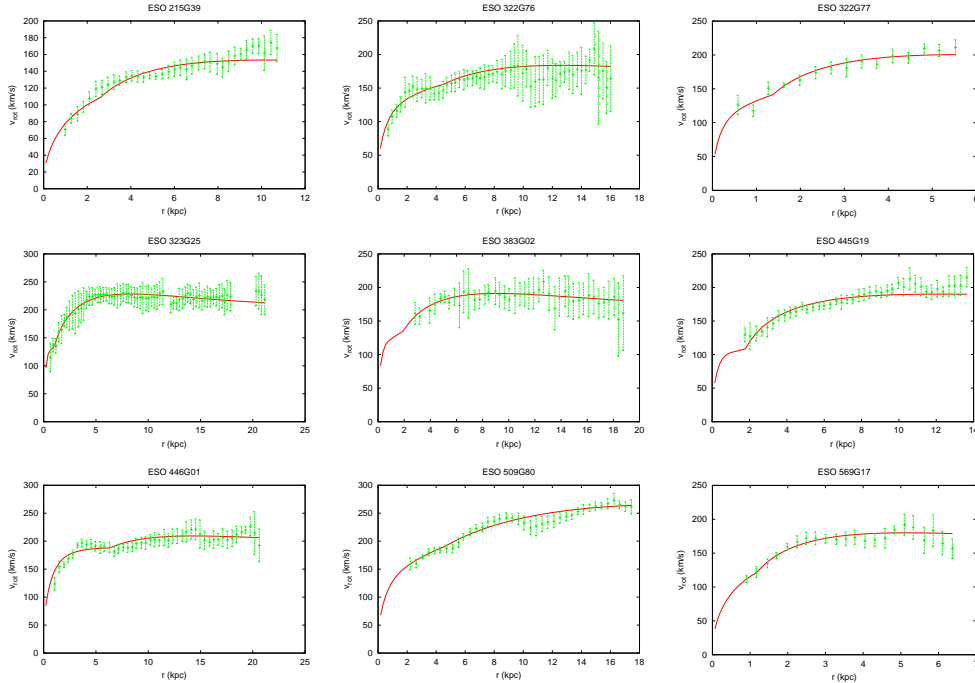


Figure 2. Best fit curves for the chosen HSB galaxies compatible with the spherical symmetry assumption, the baryonic model and having sufficiently accurate rotation curve and photometric data available. In the baryonic matter dominated radial range $r < r_b$ the model curves bend as determined by the photometric data, shown in Table 3, together with the Weyl parameters of the model. The discontinuity in the first derivative of the model curves indicate the bulge radius r_b .

established by de Blok et al. (2001). Hence we ignore the mass contributions of the stellar and gas components. At low radii $r < r_c$, the constant density implies $v^2(r) = G\rho V/r$, where V is the volume of a sphere with radius r , and $\rho = 3M_0/4r_c^3\pi$, i.e., $v \sim r$. The Weyl fluid can reproduce this behavior if we choose the equation of state $p(\mu) = 0$ (i.e. $a = 2$ and $B = 0$ in Eq. (47)). Then the dark anisotropic stress/pressure also vanishes ($P = 0$), and the remaining part of the Weyl fluid energy momentum tensor (as $Q_\mu = 0$) then represents radiation. Using Eqs. (51) - (52), (55) - (56) and (60) - (62), for $C_2 = 0$ the tangential velocity, given by Eq. (63), yields to $v_{tg}^2 \approx \gamma r^2$, the desired behavior. For $r > r_c$ we use Eq. (76), without baryonic matter ($M_b^{tot} = 0$), and apply a new notation: $M_0^{tot} = M_0$. Requiring the continuity of the rotation velocity through $r = r_c$ we have

$$v_{tg}^2(r) = \frac{GM_0}{r} \left(\frac{r}{r_c}\right)^3 [1 - H_k(r_c)] + \left\{ \frac{GM_0}{r} + c^2\beta \left[1 - \left(\frac{r_c}{r}\right)^{1-\alpha}\right] \right\} H_k(r_c), \quad (87)$$

where $H_k(r_c)$ is the logistic function given by Eq. (85).

We test the model with a sample of 9 LSB galaxies, extracted from a larger sample from de Blok & Bosma (2002) as typical galaxies exhibiting the plateau region. We fit Eq. (87) with the rotation curve data taken from combined HI and $H\alpha$ measurements. The fitted curves are represented on Fig. 3. In all cases we find remarkably good agreement between the model and observations. Outside the core radius the parameters of the equation of state a and B are determined by fitting through α and β (see Section 5).

From a χ^2 -test we determine M_0 and r_c , and also the Weyl parameters α and β , shown on Table 4 and on Fig. 4.

8 DISCUSSIONS AND FINAL REMARKS

The shape of the observed rotation curves strongly indicate the need for dark matter or equivalent modifications of gravity on galactic scale and above. However there are no universally accepted candidates explaining the whole amount of dark matter needed for agreement with observations. Because dark matter does not interact with ordinary matter, except gravitationally, the question comes whether dark matter is rather an effect of modified gravity. We have investigated whether extra dimensions could provide this type of modification in the simplest, codimension one brane-world scenario. We have derived an analytical expression for the rotational velocity of a test particle on a stable circular orbit in the exterior region to a galaxy, with Weyl fluid contributions (the dark pressure and dark radiation) included. For this we have assumed a linear equation of state for the Weyl fluid and we have argued for the rightness of this as follows.

In subsection 4.1 we have derived a system of two first order differential equations for three brane variables with straightforward geometrical meaning. These variables are: (1) the acceleration of the normal congruence to the $t=\text{const}$ hypersurfaces; (2) the expansion of the normal congruences to the $r=\text{const}$ spheres in the $t=\text{const}$ hypersurfaces; and (3) the scalar characterizing the electric part of the Weyl curvature of the brane (due to its construction, this is defined

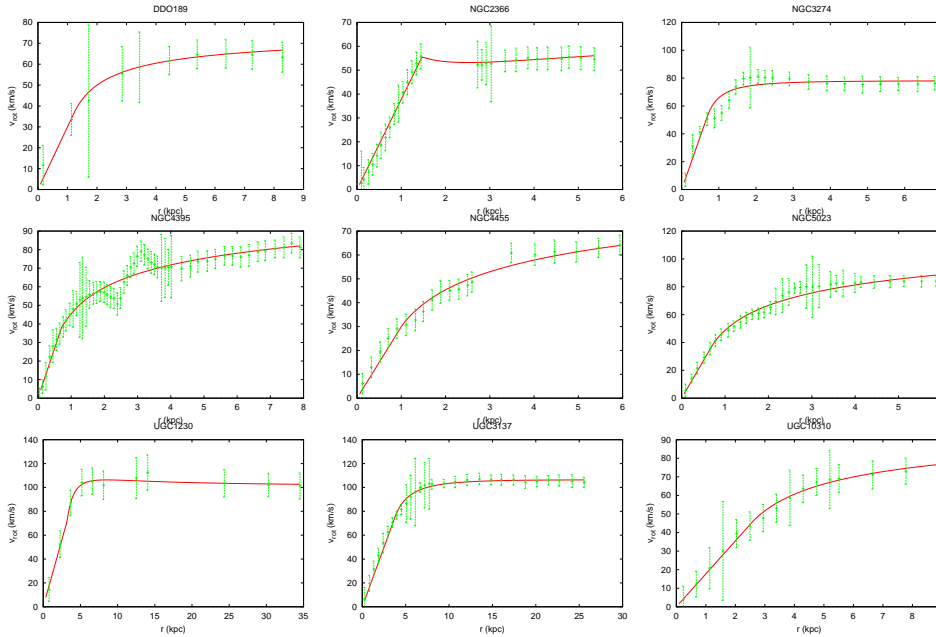


Figure 3. Best fit curves for the LSB galaxy sample. The parameters of the model velocity curves are given in Table 4.

on the $t=\text{const}$ hypersurfaces). The dark pressure and dark radiation do not enter these equations.

We also derived additional algebraic relations for these three quantities valid in Schwarzschild space-time. As the brane-world spherically symmetric space-time is a modification of the Schwarzschild solution, we have slightly modified one of these relations (by introducing two continuous deformation parameters, which take the value 1 for Schwarzschild), closing in this way the system of equations for these variables. The Cauchy-Peano theorem then proves the existence of a solution for this system.

We have shown then, how the dark pressure and dark radiation are determined algebraically in terms of the above mentioned two kinematical and one brane Weyl quantities. We find that the above mentioned choice induces a linear relation between them, the desired equation of state.

There are two types of evolutions, which in principle could destroy this solution. No problem is posed by the temporal evolution, due to the static character of the space-time. On the other hand, the above determined solution of the brane equations stands as a set of "initial" conditions for the system of first order off-brane evolution (propagation) equations (for example along some suitably defined parameter associated to the brane normal). This in turn again allows for solutions due to the Cauchy-Peano theorem. Thus we only have to check then, whether such initial conditions are allowed, in other words whether there is any constraint involving these initial conditions, which has to be obeyed. Such a constraint indeed exists: it is the 4-dimensional (twice contracted) Bianchi identity on the brane. This identity however trivially follows from the equations solved before, therefore the linear equation of state is compatible with both types of evolution.

The model has several free parameters, which in principle could be fixed in such a way to explain the observed galactic rotation curve behavior.

In order to much closely test this assumption, we have considered a sample of 9 HSB and 9 LSB galaxies with well measured combined HI and $H\alpha$ rotation curves. Since LSB galaxies are known to be dark matter dominated (McGaugh et al. (2001)), reproducing their rotation curves without the need of any dark matter component would be a major achievement. Fitting the model to rotation curve data and photometric measurements allowed us to constrain the Weyl parameters α and $\beta = -C$; also determine the mass-to-light ratios M/L of the baryonic components in HSB galaxies, and the total core mass M_0 and radius r_c of LSB galaxies. The fit was in all cases within 1σ confidence level, which supports the choice of the equation of state (46) from a physical point of view. In all cases we found $\beta \ll 1$ and in most cases $\alpha \in (0.4, 0.9)$, which for the constants $\mathcal{A} = (1 + \alpha)/2$, $\mathcal{B} = \mathcal{A}(1 - \beta) + \alpha\beta$ introduced in Section 4.1 give $\mathcal{A} \approx \mathcal{B} \in (0.7, 0.95)$. These express the difference of our model from a Schwarzschild solution, for which $\mathcal{A} = \mathcal{B} = 1$.

With the parameters determined from the fit the theoretical rotation curves will have an almost flat (slightly increasing) asymptotic behavior at larger radii than the available observations of HI and $H\alpha$ velocities for these galaxies. This tendency is somewhat contradictory with the shape of the universal rotation curve, scaling only with the virial mass (Salucci et al. 2007), at least for the well-fitting model parameters. The asymptotic shape of the universal rotation curve shows a decreasing tendency, as has been found from N-body simulations, which assume the Navarro-Frenk-White CDM model (Navarro et al. 1996). We note though that parameters of the Weyl fluid reproducing the asymptotics of the universal rotation curve can be found, but for these the fit with the HI and $H\alpha$ velocity data falls outside 3σ confidence level.

Observationally, the galactic rotation curves remain flat to the farthest distances that can be observed. On the other

hand there is a simple way to estimate an upper bound for the cutoff of the constancy of the tangential velocities. The idea is to consider the point at which the decaying density profile of the dark radiation associated to the galaxy becomes smaller than the average energy density of the Universe. Let the value of the coordinate radius at the point where the two densities are equal be R_U^{\max} . Then at this point $3\alpha_b U (R_U^{\max}) = (8\pi G/c^2) \rho_{univ}$, where $\rho_{univ} c^2$ is the mean energy density of the Universe. In the limit of large r , with the use of Eq. (72), we can approximate the dark radiation term as $3\alpha_b U \approx v_0/r^2$. Hence for R_U we obtain

$$R_U^{\max} = c \sqrt{\frac{v_0}{8\pi G \rho_{univ}}}. \quad (88)$$

The mean density of the Universe is given by $\rho_{univ} = \rho_{crit} = 3H_0^2/8\pi G$, where H_0 is the Hubble constant, given by $H_0 = 100h$ km/sec Mpc, $1/2 \leq h \leq 1$. Therefore

$$R_U^{\max} \approx c H_0^{-1} \sqrt{\frac{v_0}{3}} \approx 3 \times 10^3 \times \sqrt{\frac{v_0}{3}} h^{-1} \text{ Mpc}. \quad (89)$$

A numerical evaluation of R_U^{\max} requires the knowledge of the constant v_0 in the flat region, and of the basic fundamental cosmological parameters. In the case of the HSB galaxies $v_0 \in (0.237 \times 10^{-6}, 0.63 \times 10^{-6})$, while in the case of the LSB galaxies, $v_0 \in (0.316 \times 10^{-7}, 0.316 \times 10^{-6})$. This gives for R_U^{\max} a range of $R_U^{\max} \in (0.84h^{-1} \text{ Mpc}, 1.37h^{-1} \text{ Mpc})$ for the HSB galaxies, and $R_U^{\max} \in (0.307h^{-1} \text{ Mpc}, 0.97h^{-1} \text{ Mpc})$ for the LSB galaxies, respectively. The measured flat regions are about $R \approx 2 \times R_{opt}$, where R_{opt} is the radius encompassing 83% of the total integrated light of the galaxy (Binney & Tremaine 1987; Persic et al. 1996; Borriello & Salucci 2001). If we take as a typical value $R \approx 30$ kpc, then it follows that $R \ll R_U^{\max}$. However, according to our model, the flat rotation curves region should extend far beyond the present measured range.

An alternative estimation of R_U^{\max} can be obtained from the observational requirement that at the cosmological level the energy density of the dark matter represents a fraction $\Omega_m \approx 0.3$ of the total energy density of the Universe $\Omega = 1$. Therefore the dark matter contribution inside a radius R_U^{\max} is given by $4\pi\Omega_m (R_U^{\max})^3 \rho_{crit}/3$, which gives

$$R_U^{\max} \approx \sqrt{\frac{1}{2\Omega_m} \frac{c}{H_0}} \left(\frac{v_{tg}}{c} \right). \quad (90)$$

Therefore, by assuming that the dark radiation contribution to the total energy density of the Universe is of the order of $\Omega_m \approx 0.3$ we have $R_U^{\max} \in (388h^{-1}, 3881h^{-1})$ kpc for $v_{tg} \in (10^{-4}, 10^{-3})$.

The limiting radius at which the effects of the extra-dimensions extend, far away from the baryonic matter distribution, is given in the present model by Eqs. (89) or (90). In the standard dark matter models this radius is called the truncation parameter s , and it describes the extent of the dark matter halos. Values of the truncation parameter by weak lensing have been obtained for several fiducial galaxies by Hoekstra et al. (2004). In the following we compare our results with the observational values of s obtained by fitting the observed values with the truncated isothermal sphere model, as discussed in some detail in Hoekstra et al. (2004). The truncation parameter s is related to R_U^{max} by the re-

lation $s = R_U^{max}/2\pi$ (see Eq. (4) in Hoekstra et al. (2004)). Therefore, generally s can be obtained from the relation

$$s \approx \frac{\sigma}{\sqrt{6}\pi} \sqrt{\frac{1}{2\Omega_m}} H_0^{-1}, \quad (91)$$

where σ is the velocity dispersion, expressed in km/s. Hence the truncation parameter is a simple function of the velocity dispersion and of the cosmological parameters only. For a velocity dispersion of $\sigma = 146$ km/s and with $\Omega_m = 0.3$, Eq. (91) gives $s \approx 245h^{-1}$ kpc, while the truncation size obtained observationally in Hoekstra et al. (2004) is $s = 213h^{-1}$ kpc. For $\sigma = 110$ km/s we obtain $s \approx 184h^{-1}$ kpc, while $\sigma = 136$ km/s gives $s \approx 228h^{-1}$ kpc. All these values are consistent with the observational results reported in Hoekstra et al. (2004), the error between prediction and observation being of the order of 20%. We have also to mention that the observational values of the truncation parameter depend on the scaling relation between the velocity dispersion and the fiducial luminosity of the galaxy. Two cases have been considered in Hoekstra et al. (2004), the case in which the luminosity L_B does not evolve with the redshift z and the case in which L_B scales with z as $L_B \propto (1+z)$. Depending on the scaling relation slightly different values of the velocity dispersion and truncation parameter are obtained.

One of the most straightforward evidence for dark matter comes from the radial Tully-Fisher relation (Yegorova & Salucci 2007): at a given galactocentric distance (measured in unit of the optical radius) there is a relation between rotation velocities and the absolute magnitudes of the galaxies. From this relation we can extract information about the mass distribution of spiral galaxies. We have studied whether the Weyl model satisfies this relation. The plot on Fig. 5 is in good agreement with the result of Yegorova & Salucci (2007).

Statistical studies of N-body simulations reveal that there is a link between halo masses and galaxy properties (e.g. luminosity, baryonic mass) (Shankar et al. 2006; Moster et al. 2010). We have compared the equivalent halo mass predicted by the Weyl model M_{Weyl} with the halo mass arising from the simulations, $M_{simulation}$ (Moster et al. 2010) (5). From the baryonic mass $M_b(\infty) + M_d(\infty)$ we have derived the predicted halo mass $M_{simulation}$ with Eq. (2) in Moster et al. (2010). With this mass we have calculated the virial radius of the galaxy R_{vir} (see Eq. (4) in Salucci et al. (2007)) and the Weyl halo mass, defined as

$$M_{Weyl} = c^2 \beta \left[1 - \left(\frac{r_b}{r} \right)^{1-\alpha} \right] \frac{R_{vir}}{G}. \quad (92)$$

With one exception the emerging masses are of same order of magnitude, in one case being also equal. These derived data signals some tension between the Weyl fluid model and the numerical simulations.

9 ACKNOWLEDGEMENTS

We would like to thank to the anonymous referee for comments and suggestions that helped us to significantly improve the manuscript. We acknowledge discussions with József Vinkó at an earlier stage of this work. LÁG is grateful to Tiberiu Harko for kind hospitality during his visit

[tbp]

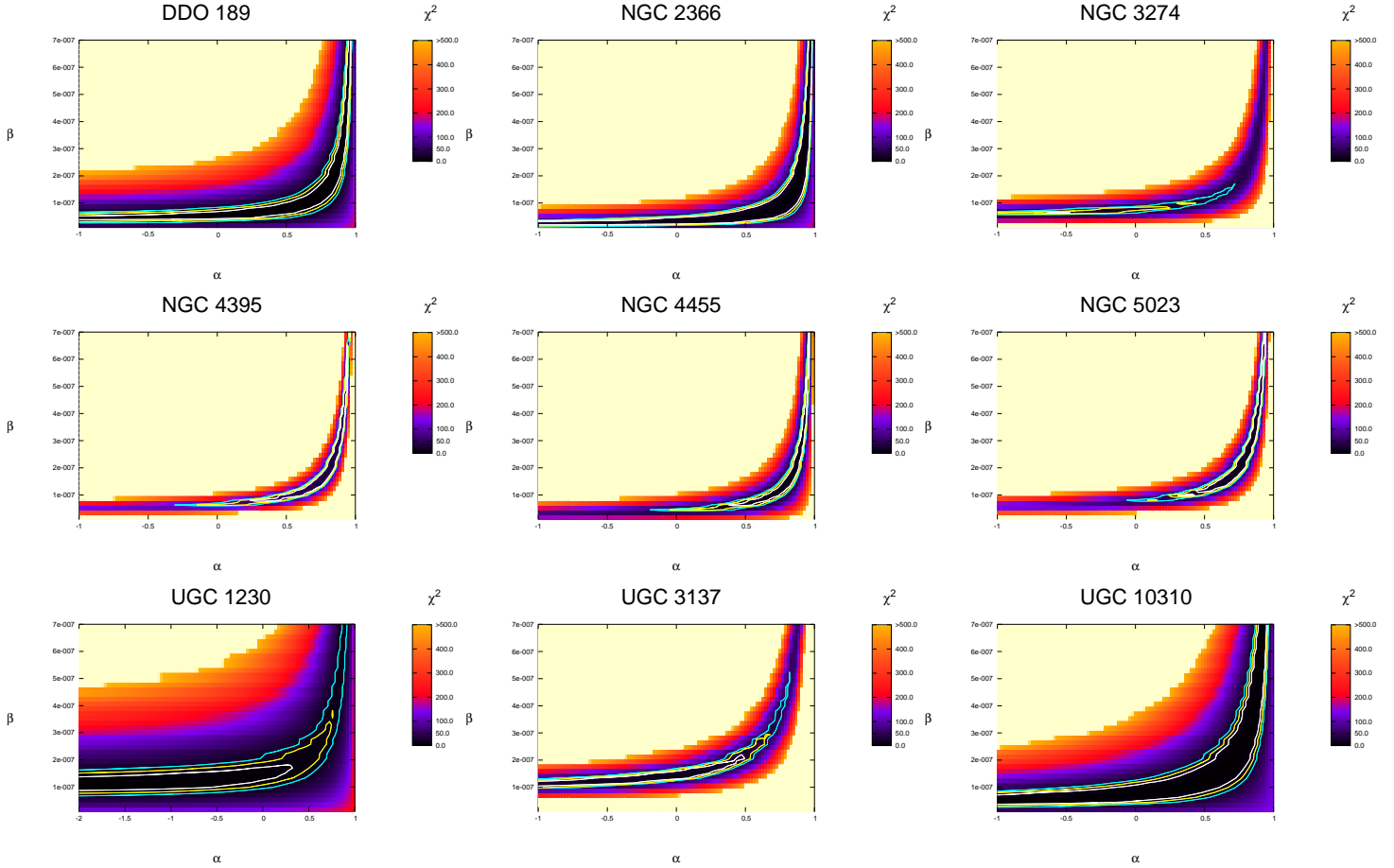


Figure 4. The fit of the rotation curves of LSB galaxies. The contours refer to the 68.3% (1σ), 95.4% (2σ) and 99.7% (3σ) confidence levels. The color code for χ^2 is indicated on the vertical stripes. The light grey vertical line denotes the forbidden region ($\alpha = 0$).

at the University of Hong Kong. LÁG and ZK were partially supported by COST Action MP0905 "Black Holes in a Violent Universe". TH was supported by the GRF grant No. 701808P of the government of the Hong Kong SAR.

APPENDIX I: 3+1+1 DECOMPOSITION OF THE 5D WEYL CURVATURE

With the brane normal n^A and the temporal normal u^B to the spatial hypersurfaces singled out, the five-dimensional Weyl tensor \tilde{C}_{ABCD} admits a 3+1+1 decomposition (Keresztes & Gergely 2010a), generalizing the corresponding decomposition of the four-dimensional Weyl tensor C_{abcd} .

The projections

$$-k_4^4 U = \tilde{C}_{ABCD} n^A u^B n^C u^D, \quad (93)$$

$$k_4^4 Q_K = \tilde{C}_{ABCD} h_K^A n^B u^C n^D, \quad (94)$$

$$-k_4^4 P_{AB} = \tilde{C}_{ABCD} h_{(K}^A n^B h_{L)}^C n^D. \quad (95)$$

of the 5-dimensional Weyl tensor combine to an effective fluid on the brane, the Weyl fluid. (Angular brackets $\langle \rangle$ on

indices denote tensors which are projected in all indices with the 3-metric $h_{IJ} = {}^{(5)}g_{IJ} - n_I n_J + u_I u_J$, symmetrized and trace-free.)

The projections

$$\mathcal{E}_{KL} = \tilde{C}_{ABCD} h_{(K}^A u^B h_{L)}^C u^D \quad (96)$$

and

$$\mathcal{H}_{KL} = \frac{1}{2} \varepsilon_{(K}{}^{AB} h_{L)}^C \tilde{C}_{ABCD} u^D \quad (97)$$

are related to the electric and magnetic parts of the four-dimensional Weyl tensor on the brane, $\tilde{E}_{ac} = C_{abcd} u^b u^d$ and $\tilde{H}_{kl} = \frac{1}{2} \varepsilon_{(k}{}^{ab} h_{l)}^c C_{abcd} u^d$, as

$$\begin{aligned} \mathcal{E}_{ab} &= E_{ab} - \frac{k_4^4}{2} P_{ab} - \frac{1}{2} \left(\hat{K} + \frac{\hat{\Theta}}{3} \right) \hat{\sigma}_{ab} \\ &\quad + \frac{1}{2} \hat{\sigma}_{c(a} \hat{\sigma}_{b)}^c + \frac{1}{2} \hat{K}_{(a} \hat{K}_{b)}, \end{aligned} \quad (98)$$

$$\mathcal{H}_{ab} = H_{ab} - \varepsilon_{(a}{}^{cd} \hat{\sigma}_{b)c} \hat{K}_d, \quad (99)$$

Here $\hat{K} = u^B u^C \tilde{\nabla}_C n_B$, $\hat{K}_A = h_A^K u^C \tilde{\nabla}_C n_K$, $\hat{\Theta} = h^{AB} \tilde{\nabla}_{AN} B$, and $\hat{\sigma}_{AB} = h_{(A}^K h_{B)}^L \tilde{\nabla}_{KN} L$ are kinematic quantities emerging as various projections of the extrinsic curva-

[tbp]

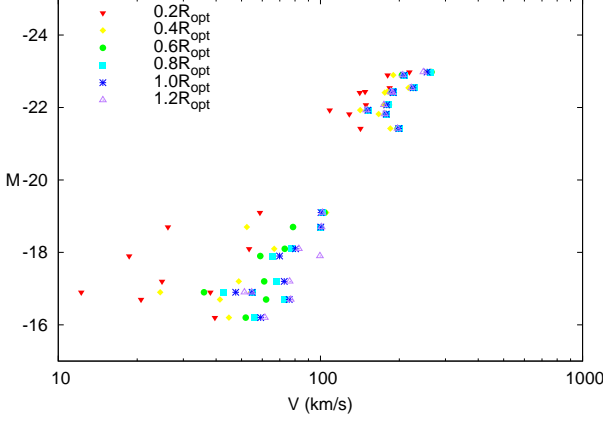


Figure 5. The radial Tully-Fisher relation of our HSB and LSB Galaxy samples: absolute magnitude of the galaxies as function of the rotational velocities predicted by the Weyl model at 0.2 (red), 0.4 (yellow), 0.6 (green), 0.8 (cyan), 1 (navy), 1.2 (lilac) optical radii.

ture of the brane ($\hat{\Theta}$ and $\hat{\sigma}_{AB}$ being the expansion and shear of the brane normal), while $\tilde{\nabla}_A$ is the covariant derivative in the 5-dimensional space-time.

The rest of the components

$$\mathcal{E}_K = \tilde{C}_{ABCD} h_K^A u^B n^C u^D, \quad (100)$$

$$\mathcal{H}_K = \frac{1}{2} \varepsilon_K^{AB} \tilde{C}_{ABCD} u^C n^D, \quad (101)$$

$$\mathcal{F}_{KL} = \tilde{C}_{ABCD} h_{(K}^A u^B h_{L)}^C n^D, \quad (102)$$

$$\hat{\mathcal{H}}_{KL} = \frac{1}{2} \varepsilon_{(K}^{AB} h_{L)}^C \tilde{C}_{ABCD} n^D \quad (103)$$

do not enter the equations on the brane.

APPENDIX II: DYNAMICS ON THE BRANE

In the 2+1+1 formalism on a brane with spherical symmetry the covariant derivative of any scalar field $f(r)$, taken along the integral curves of the radial vector field r^a is defined (Keresztes & Gergely 2010a) as $f^* = r^a D_a f$. The nontrivial dynamical equations are four ordinary differential equations:

$$\tilde{\Theta}^* + \frac{\tilde{\Theta}^2}{2} + \frac{2\tilde{E}}{3} + \frac{k_4^4}{3} (2U + P) = 0, \quad (104)$$

$$(U + 2P)^* + 4AU + (2A + 3\tilde{\Theta})P = 0, \quad (105)$$

$$A^* + A(\tilde{\Theta} + A) - k_4^4 U = 0, \quad (106)$$

$$A^* + A\left(A - \frac{\tilde{\Theta}}{2}\right) - \tilde{E} + \frac{k_4^4}{2} P = 0, \quad (107)$$

for the five variables $\tilde{\Theta}$, A , \tilde{E} , U , P . Eq. (105) is equivalent with the constraint Eq. (11). The difference of Eqs. (106) and (107) gives a simple algebraic relation between the dark radiation U , dark pressure P acceleration A of temporal normals, expansion of radial geodesics $\tilde{\Theta}$ and electric part of the 4-dimensional Weyl tensor \tilde{E} , respectively:

$$k_4^4 (2U + P) = 3A\tilde{\Theta} + 2\tilde{E}. \quad (108)$$

This enables us to eliminate the Weyl contributions from Eq. (106), obtaining

$$\tilde{\Theta}^* + \frac{\tilde{\Theta}^2}{2} + \frac{4\tilde{E}}{3} + A\tilde{\Theta} = 0. \quad (109)$$

Another algebraic relation emerges as follows. From (a) the relation between the Ricci scalar of the sphere and the Riemann tensor of the 3-space:

$$\begin{aligned} {}^2\mathcal{R} &= (h^{ac} - r^a r^c)(h^{bd} - r^b r^d) \left[{}^3\mathcal{R}_{abcd} \right. \\ &\quad \left. + (D_a r_c)(D_b r_d) - (D_a r_d)(D_b r_c) \right] \\ &= \frac{2}{3} \left[k_4^4 (U - P) - 2\tilde{E} \right] + \frac{\tilde{\Theta}^2}{2}, \end{aligned} \quad (110)$$

where we have used $D_a r_b = \tilde{\Theta}(h_{ab} - r_a r_b)/2$, (b) the 3-dimensional Riemann tensor given in Keresztes & Gergely (2010a)¹, which in the spherically symmetric case simplifies to

$$\begin{aligned} {}^3\mathcal{R}_{abcd} &= \frac{2k_4^4}{3} U h_{c[a} h_{b]d} - 2 \left(\tilde{E}_{d[a} h_{b]c} - \tilde{E}_{c[a} h_{b]d} \right) \\ &\quad - k_4^4 (P_{d[a} h_{b]c} - P_{c[a} h_{b]d}), \end{aligned} \quad (111)$$

and (c) the Gaussian curvature of the two-dimensional spacelike group orbits orthogonal to r^a and u^a being ${}^2\mathcal{R} = 2/r^2$, we obtain

$$\tilde{E} = \frac{k_4^4}{2} (U - P) + \frac{3\tilde{\Theta}^2}{8} - \frac{3}{2r^2}. \quad (112)$$

We need to relate the newly introduced curvature coordinate to the \star -derivative. For this we take the \star -derivative of Eq. (112), employ Eqs. (109), (105), (106); also the \star -derivative of Eq. (108) for eliminating \tilde{E}^* , finding

$$(\ln r^2)^* = \tilde{\Theta}. \quad (113)$$

This relation allows to replace the \star -derivative in all equations by r -derivatives, denoted by a prime. Thus Eqs. (109), (105), (106) can be rewritten as

$$\frac{r\tilde{\Theta}}{2}\tilde{\Theta}' + \frac{\tilde{\Theta}^2}{2} + \frac{4\tilde{E}}{3} + A\tilde{\Theta} = 0, \quad (114)$$

$$\frac{r\tilde{\Theta}}{2}(U + 2P)' + 4AU + (2A + 3\tilde{\Theta})P = 0, \quad (115)$$

$$\frac{r\tilde{\Theta}}{2}A' + A(\tilde{\Theta} + A) - k_4^4 U = 0, \quad (116)$$

where the prime denotes the derivative with respect to r .

In summary, the variables U , P , A , \tilde{E} and $\tilde{\Theta}$ are constrained by two independent first order ordinary differential equations (114), (116) and two algebraic equations (108), (112). Eq. (115) follows from these.

¹ We note that there is a missing factor 2 in front of \mathcal{E} in Eq. (23) of Keresztes & Gergely (2010a). The conversion of notations to the notations of the present paper is: $(\mathcal{E}, \hat{\mathcal{E}}_a, \hat{\mathcal{E}}_{ab}, E_{ab}) \rightarrow (-k_4^4 U, k_4^4 Q_a, -k_4^4 P_{ab}, \tilde{E}_{ab})$.

REFERENCES

- Albuquerque I. F. M., Baudis L., 2003, *Phys. Rev. Lett.*, 90, 221301
- Bekenstein J. D., 2004, *Phys. Rev. D*, 70, 083509
- Bernal A., Siddhartha Guzman F., 2006, *Phys. Rev. D*, 74, 063504
- Bertolami O., Böhmer C. G., Harko T., Lobo F. S. N., 2007, *Phys. Rev. D*, 75, 104016
- Biermann P. L., Kusenko A., 2006, *Phys. Rev. Lett.*, 96, 091301
- Binney J., Tremaine S., 1987, *Galactic dynamics*, Princeton University Press, Princeton
- Bothun G. D., Schombert J. M., Impey C. D., Sprayberry D., McGaugh S. S., 1993, *AJ*, 106, 530
- Böhmer C. G., Harko T., 2007a, *Month. Not. Roy. Astr. Soc.*, 379, 2007
- Böhmer C. G., Harko T., 2007b, *JCAP*, 0706, 025
- Böhmer C. G., Harko T., 2007c, *Class. Quant. Grav.*, 24, 3191
- Böhmer C. G., Harko T., Lobo F. S. N., 2008, *Astropart. Phys.*, 29, 386
- Boriello A., Salucci P., 2001, *Month. Not. Roy. Astr. Soc.*, 323, 285
- Briscese F., 2011, *Phys. Lett. B*, 696, 315
- Brownstein J. R., Moffat J. W., 2006, *Astrophys. J.*, 636, 721
- Dadhich N., Maartens R., Papadopoulos P., Rezanian, V., 2000, *Phys. Lett. B*, 487, 1
- de Blok W. J. G., McGaugh S.S., Bosma A., Rubin V., 2001 *Astrophys. J.*, 552, L23-L26
- de Blok W. J. G., Bosma A., 2002, *Astron. Astrophys.* 385, 816
- Fuchs B., Mielke E. W., 2004, *Month. Not. Roy. Astr. Soc.*, 350, 707
- Freeman K. C., 1970, *Astrophys. J.*, 160, 811
- Gergely L. Á., 2003 *Phys. Rev. D*, 68, 124011
- Gergely L. Á., 2006 *Phys. Rev. D*, 74, 024002
- Gergely L. Á., 2007 *JCAP*, 07, 027
- Gergely L. Á., 2008 *Phys. Rev. D*, 78, 084006
- Gergely L. Á., 2009 *Phys. Rev. D*, 79, 086007
- Horváth Z., Gergely L. Á., Hobill D., 2010 *Class. Quantum Grav.*, 27, 235006
- Germani C., Maartens R., 2001, *Phys. Rev. D*, 64, 124010
- Giannios D., 2005, *Phys. Rev. D*, 71, 103511
- Guzmán F. S., Ureña-López L. A. 2006, *Astrophys. J.*, 645, 814
- Giovannelli R., Haynes M. P., Salzer J. J., Wegner G., da Costa L. N., Freudling W., 1994, *Astronomical Journal*, 107, 2036
- Harko T., Mak M. K., 2004, *Phys. Rev. D*, 69, 064020
- Harko T., Mak M. K., 2005, *Annals of Physics*, 319, 471
- Harko T., Cheng K. S., 2006, *Astrophys. J.*, 636, 8
- Harko T., 2011, eprint arXiv:1101.3655
- Hernandez X., Matos T., Sussman R. A., Verbin, Y., 2004, *Phys. Rev. D*, 70, 043537
- Hoekstra H., Yee H. K. C., Gladders M. D., 2004, *Astrophys. J.*, 606, 67
- Kannappan S. J., Gawiser E., 2007, *Astrophys. J.*, 657, L5
- Keresztes Z., Gergely L. Á., *Class. Quant. Grav.*, 27, 105009
- Keresztes Z., Gergely L. Á., 2010 *Ann. Physik*, 19, 249
- Landau L. D., Lifshitz E. M., 1975, *The Classical Theory of Fields*, Pergamon Press, Oxford
- Maeda K., Mizuno S., Torii, T., 2003, *Phys. Rev. D*, 68, 024033
- Mak M. K., Harko, T., 2004, *Phys. Rev. D*, 70, 024010
- Mannheim P. D., 1997, *Astrophys. J.*, 479, 659
- Maartens R., Koyama K., 2010, *Living Reviews in Relativity*, 13, 5
- Matos T., Guzman F. S., Nunez, D., 2000, *Phys. Rev. D*, 62, 061301
- McGaugh S.S., Rubin V., de Blok W.J.G., 2001, *Astron. J.* 122, 2381
- Milgrom M., 1983, *Astrophys. J.*, 270, 365
- Moffat J. W., Sokolov I. Y., 1996, *Phys. Lett. B*, 378, 59
- Moster B. P., Somerville R. S., Maulbetsch C., van den Bosch F. C., Maccio A. V., Naab T., Oser L., 2010, *Astrophys. J.*, 710, 903
- Munyanza F., Biermann P. L., 2006, *Astron. Astrophys. Letters*, 458, L9
- Navarro J. F., Frenk C. S., White, S. D. M., 1996, *Ap. J.* 462, 563
- Nucamendi U., Salgado M., Sudarsky D., 2001, *Phys. Rev. D*, 63, 125016
- Overduin J. M., Wesson, P. S., 2004, *Phys. Repts.*, 402, 267
- Pal S., Bharadwaj S., and Kar S., 2005, *Phys. Lett. B*, 609, 194
- Pal S., 2008, *Phys. Rev. D*, 78, 043517
- Palunas, P., Williams, T. B., 2000, *Astron. Journal*, 120, 2884
- Persic M., Salucci P., Stel, F., 1996, *Month. Not. Roy. Astr. Soc.*, 281, 27
- Portinari L., Sommer-Larsen J., Tantalo, R., 2004, *Month. Not. Roy. Astr. Soc.*, 347, 691
- Randall L., Sundrum R., 1999a, *Phys. Rev. Lett.*, 83, 3370
- Randall L., Sundrum R., 1999b, *Phys. Rev. Lett.*, 83, 4690
- Rahaman F., Kalam M., DeBenedictis A., Usmani A. A., Ray S., 2008, *Month. Not. Roy. Astr. Soc.*, 389, 27
- Roberts M. D., 2004, *Gen. Rel. Grav.*, 36, 2423
- Salucci P., Lapi A., Tonini C., Gentile G., Yegorova I., Klein U., 2007, *Month. Not. Roy. Astr. Soc.*, 378, 41-47
- Sanders R. H., 1984, *Astron. Astrophys.*, 136, L21
- Sasaki M., Shiromizu T., Maeda K., 2000, *Phys. Rev. D*, 62, 024008
- Sérsic J. L., 1968, *Atlas de Galaxias Australes*, Cordoba, Argentina, Observatorio Astronomico
- Shankar F., Lapi A., Salucci P., De Zotti G., Danese L., 2006, *Astrophys. J.*, 643, 14
- Shiromizu T., Maeda K., Sasaki M., 2000, *Phys. Rev. D*, 62, 024012
- Thuan T. X., Gott J. R., Schneider S. E., 1987, *Astrophys. J. (Letters)*, 315, L93
- van der Hulst J. M., Skillman E. D., Smith T. R., Bothun G. D., McGaugh S. S., de Blok, W. J. G., 1993, *AJ*, 106, 548
- Wiseman T., 2002, *Phys. Rev. D*, 65, 124007
- Yegorova I. A., Salucci P., 2007, *Month. Not. Roy. Astr. Soc.* 377, 507